UNIVERSIDAD POLITÉCNICA DE MADRID

ESCUELA TÉCNICA SUPERIOR
DE INGENIEROS DE TELECOMUNICACIÓN

GRADO EN INGENIERÍA DE TECNOLOGÍAS Y SERVICIOS DE TELECOMUNICACIÓN

TRABAJO FIN DE GRADO

DESIGN AND IMPLEMENTATION OF A LINEAR ACTUATOR BASED ON THE LORENTZ FORCE

DANIEL GALERA NEBOT

2019

UNIVERSIDAD POLITÉCNICA DE MADRID

ESCUELA TÉCNICA SUPERIOR
DE INGENIEROS DE TELECOMUNICACIÓN

Reunido el tribunal examinador en el día de la fecha, constituido por

Presidente:	Dr.
Vocal:	Dr.
Secretario:	Dr.
Suplente:	D.

para juzgar el Trabajo Fin de Titulacin titulado:

DESIGN AND IMPLEMENTATION OF A LINEAR ACTUATOR BASED ON THE LORENTZ FORCE

del alumno D. DANIEL GALERA NEBOT
dirigido por Dr. Álvaro Gutiérrez Martín
del Departamento de Tecnología Fotónica y Bioingeniería

Acuerdan otorgar la calificación de: ____________________________

Y, para que conste, se extiende firmada por los componentes del tribunal, la presente diligencia

Madrid, DIA de mes de AÑO

El Presidente	El Vocal	El Secretario
Fdo: ____________________	Fdo: ____________________	Fdo: ____________________

UNIVERSIDAD POLITÉCNICA DE MADRID

ESCUELA TÉCNICA SUPERIOR
DE INGENIEROS DE TELECOMUNICACIÓN

GRADO EN INGENIERÍA DE TECNOLOGÍAS Y SERVICIOS DE TELECOMUNICACIÓN

TRABAJO FIN DE GRADO

DESING AND IMPLEMENTATION OF A LINEAR ACTUATOR BASED IN LORENTZ FORCE

DANIEL GALERA NEBOT

2018

Abstract

Nowadays, the implementation of artificial muscles that mimic natural muscles is a pending task. One way to implement those muscles is by mimicking myocites , the cells which compound the muscles. In the market, there are several commercially available electric actuators that can be considered to act as these cells. However, these actuators have to be small enough to compound a reasonable size. Solenoid valves were chosen as a first approximation because they are the littlest linear electric actuators with significant stroke in market. Unfortunately, solenoid's energy consumption, heat dissipation and deterioration in long duty cycles lead to the necessity of developing a linear actuator suitable for mimicking muscles.

In this thesis, the Lorentz force has been chosen as the physical principle which would generate motion and some designs has been tested to exploit that force to mimic myocites. Preliminary tests lead to define some concepts and conditions to seize the Lorentz force in a linear actuator. The actuators based on these ideas are proposed to be named **Lorentzito**.

After a theoretical analysis, two different implementations are constructed and measured. Only one was suitable to seize the Lorentz force. Some phenomenons were identified as possible reasons for the differences observed between the two implementations and between the theoretical analysis and real measurements. To compare different implementations of the Lorentzito with other technologies, several parameters have been defined. Those parameters were considered as figures of merit and were optimized by varying the size and electric current.

In summary, this thesis shows that the Lorentz force can be used as a source of motion suitable for mimicking myocites. Therefore, a new way for building artificial muscles is incorporated to the state of the art.

Resumen

A día de hoy, la implementación de músculos artificiales que imitan los músculos biológicos no está resuelta. Una maenra de hacerlo es imitando las células que componen dichos músculos, los miocitos. El comportamiento de algunos acutadores eléctricos en el mercado podría llegar a ser identificados con el de estas células. Estos actuadores tendrían que ser sufcientemente pequeños para agruparse sin ocupar demasiado espacio. Las válvulas hechas con solenoides se tomaron como una primera aproximación por ser actuadores lineales eléctricos con suficiente carrera y suficientemente pequeños. Sin embargo, su consumo energético, la disipación de calor, y su desgaste en largos cilos de trabajo señaló la necesidad de desarrollar un actuador lineal adecuado para imitar músculos.

En este trabajo, la fuerza de Lorentz se ha elegido como el principio físico para generar movimiento y algunos diseños se han probado para usar esta fuerza para imitar a los miocitos. Los tests preliminares llevaron a definir algunos conceptos y condiciones para poder aprovechar la fuerza de Lorentz en un actuador lineal. Para los actuadores basados en estas ideas se propone el nombre de **Lorentzito**.

Tras una análisis teórico, se han implementado y medido dos prototipos. Tan solo uno fue adecuado para aprovechar la fuerza de Lorentz. Algunos fenómenos fueron identificados como posibles motivos de las diferencias observadas entre ambas implementaciones y el análisis teórico y las medidas. Para comparar el Lorentzito con otras tecnologías equivalentes, algunos parámetros fueron definidos. Estos parámetros fueron considerados como figuras de mérito y optimizados respecto al tamaño y la corriente eléctrica.

En resumen, este trabajo muestra que la fuerza de Lorentz puede ser usada como una fuente de movimiento capaz de imitar a los miocitos. Por tanto, introduce una nueva manera de construir músculos artificiales al estado del arte.

Key Words

Lorentz force ; Halbach configuration ; artificial muscle ; bioinspired ; Lorentzito ; liquid electrical conduction ; linkage problem ; nerve-cell-tendon model

Acknowledgment

Although this thesis has been mainly developed in Laboratorio de Robótica y Control de la E.T.S de Ingenieros de Telecomunicación, I thank to CEMDATIC and Rama de Estudiantes del IEEE de la ETSIT the time I have shared with its members.

I also say thank you to all those who have share with me part of their time hearing, testing or correcting ideas and science present in this thesis. Some names are: Álvaro Gutiérrez Martín, Jorge Galera Nebot, Manuel Caño-Garcia, Luis Alberto Gómez López, Andrés Velasco Santiago, Paula Nebot Mateos, Ricardo Sanz Retuerta, Ignacio López Paniagua, Carlos Santos Rancaño, Adrián García Espinosa, Carlos Cuenca Enrique, Daniel Montesano, Amadeo de Gracia Herranz, Álvaro Rodríguez Ávila.

Contents

List of Figures

Tables index

Glossary

In order of appearance

$\vec{F}$ Vectorial force.

q Electric charge value.

$\vec{E}$ Electric field.

$\vec{v}$ Velocity.

$\vec{B}$ Magentic field, also known as magnetic flux induction and magnetic flux density.

$\vec{I}$ Electric current.

$\vec{u}$ Unit vector.

A Area.

μ Magnetic permeability.

μ_0 Magnetic permeability of vacum.

l Lenght.

n Density of turns per lenght.

λ Stretch ratio.

ν Friction coeficient.

$\vec{M}$ Magnetization.

$\vec{\phi}$ Azimuth coordinate of the cylindrical coordinates.

$\vec{\rho}$ Radial coordinate of the cylindrical coordinates.

$\vec{y}$ Coordinate of the Cartesian coordinates.

$\vec{x}$ Coordinate of the Cartesian coordinates.

$NdFeB$ Alloy of neodymium, iron and boron to form the $Nd_2Fe_{14}B$ tetragonal crystalline structure.

R Electrical resistance.

P Power.

σ Electical conductivity.

PLA Polylactic acid.

NaK Eutectic mixture consists of 77% potassium and 23% sodium.

$PTFE$ Polytetrafluoroethylene.

BAM Chemical compound of aluminium, magnesium and boron $Al_{0.75}Mg_{0.75}B_{14}$.

$\rho_{\frac{N}{W}}$ Force-consumption quotient.

ρ_m Mass quotient.

g Acceleration of gravity on earth at sea level.

a_m Actuators mass.

c_D Mass density of the inner conductor.

ρ Force-mass-consumption quotient.

ϵ_v Volume efficiency coefficient.

c_v Inner conductors volume.

a_v Actuators volume.

ϵ_m Mass efficiency coefficient.

c_m Inner conductor mass.

t Time.

μ_r Relative magnetic permeability.

$\vec{J}$ Current density.

Chapter 1

Introduction and objectives

1.1 Motivation

In technological solutions of motion, servos, stepper motors, and motors are commonly used. Circular actuators prevail even when an adapter is necessary to generate a non circular motion. On the contrary, in nature, the core of motility usually starts with a contractive behaviour (**?**). Contraction, which is fundamentally a linear movement, is the main strategy to generate movement in multi-cellular beings. Among those, free rotation has only been found in digestive systems of bivalves and gastropods (**?**). This is the only biological structure found in animals that behaves similar to a motor, and it has not a motion purpose. Nevertheless, at a molecular scale, flagella motors are a common solution to motion that can be considered as a circular actuator. This structure (**?**) is widely used by unicellular beings but it does not have a counterpart in multicellular systems. That lack of rotating locomotion has been previously discussed (**??**) showing that wheels are less efficient in order to accomplish movements in complex and unpredictable terrain. It suggests that using rotatory actuators could not be the best option to move structures bigger than cells and maybe only historical reasons had lead us to develop general purpose machines with this kind of actuators. On the contrary, muscles are the most common tissues found in animals that perform a contraction with a motility purpose. Even when muscles are not present in metazoa, other contractive structures are used to generate a contraction. Examples of those structures are found in Porifera (**?**) and Placozoa (**??**).

It is undeniable that rotatory actuators are highly efficient in solving many problems. However, in general purpose machines or adaptable robots, which must operate in nature, it seems advisable to test contraction solutions as the basis of motion (**??**). In most animals, contraction starts in myocytes grouped in tissues that compound muscles. In this thesis, this scheme will be imitated to attempt motility based on contraction. This inspiration leads to solutions that need the counterpart of the myocytes, which will build up artificial contractible tissues.

Many technologies have been developed inspired by nature, most of them focusing on the concept of linear or bending actuators. Soft robotics (**???**) is a promising area which imitates the natural way of motion that could be commonly used in future robotics applications. They can perform precise and powerful movements (**?**).

Hyper-redundant robotics are also present in bio-mimetic robotics (**?**). Nevertheless, those structures act as the whole muscle imitating the functionality rather than the internal structure. Thermal driven actuators (**?**) and electroactive polymers (**?**) generate movement due to their internal structure. However, electroactive polymers are still limited by their degradation (**?**) and thermal driven actuators which have been implemented successfully in muscle-mimicking technologies (**?**) are slower than magnetic actuators such as electric motors.

In order to adapt the advantages of magnetic actuators to a contractive structure based on contractive building blocks, solenoid valves are the sole commercial option available. Small solenoids were tested in a first approximation to the myocytes approach. However, small solenoids have different problems: a continuous usage heats the core, bending it and generating malfunctioning unless the component is refrigerated. Moreover, many little solenoids cannot lift their own weight and all sizes present a high energy consumption. Those characteristics make clear that solenoid valves are not suitable to be hyper-redundant actuator in robotics. Therefore, because no commercial actuators are found to be suitable, the first step to achieve the building block of an artificial muscle is to design the myocytes counterpart.

In consequence, the aim of this thesis is to design a small, simply, reliable and stackable actuator considered as a building block. This block is intended to be part of bigger and more complex actuators mimicking the biological muscle structure with the idea of implementing ad-hoc artificial muscles. Linear motion has been chosen because of its similarities with contractive behaviour of muscle cells. Hence, the actuator will act as a myocyte. To generate force and motion, the Lorentz force, specifically the magnetic term, has been chosen because it only needs moving electrons and a magnetic field ($\vec{B}$). Both components are easy to get from electric currents and magnets.

1.2 Lorentz force

The implementation of the actuator is based on the Lorentz Force (see Equation 1.1).

$$\vec{F} = q\vec{E} + q\vec{v} \times \vec{B} \tag{1.1}$$

where q is electric charge, $\vec{E}$ is electric field in the position of the charge, $\vec{v}$ is the linear velocity of the charge and $\vec{B}$ is the magnetic field in the position of the charge. Some considerations have been taken into account to simplify the description. The current $\vec{I}$ will be used instead of q and $\vec{v}$. Being l the length through which the current flows: $q\vec{v} = l\vec{I}$. The term $q\vec{E}$ is not used to generate force in this application, then it will be considered zero in any force analysis. $\vec{B}$ and $\vec{I}$ will always be orthogonal in order to achieve the highest force. Therefore, $\vec{I} \times \vec{B} = IB\vec{u}$, being $\vec{u}$ an orthogonal unitary vector. By the previous assumptions, the Lorentz force is simplified as follows:

$$\vec{F} = IBl\vec{u} \tag{1.2}$$

1.3 Magnetic force vs Lorentz force based actuators

When the objective is to obtain force from a magnetic field, there are two options: using the attraction between magnets or using the Lorentz force. To generate a force from a controlled electric current, there are three different electromagnetic phenomena that can be exploited: the Coulomb, magnetic and Lorentz forces. Magnetic force has more applications in electric actuators. Therefore, in this thesis Lorentz force will be only compared with magnetic force and Coulomb force will be considered out of the scope of this thesis.

A magnetic force is present when the magnetic field of two different elements shares a common space. These magnetic fields can be originated in ferromagnetic, paramagnetic o diamagnetic materials when excited from an external magnetic field. Magnetic fields can also be produced by electric currents in vacum and magnetized materials with a significant remanence. In an actuator based on magnetic forces, those fields must be controlled. Therefore, an electric current will be needed either to generate the field by itself or to excite a material with magnetic properties. The Lorentz force also needs an electric current to have a non zero value. Those currents that will control the actuation must be applied from an external power source, so both methods can be compared in terms of power consumption. It will be demonstrated that using the magnetic force is, in some sizes, worse than using the Lorentz force in a relevant aspect, energy efficiency.

Both forces, the Lorentz force and the magnetic force, depend directly of magnetic field ($\vec{B}$) so high fields with low energy consumption are desirable. The magnetic field ($\vec{B}$), is related to the magnetic field intensity ($\vec{H}$) by magnetic permeability (μ). To activate a force between magnets, the magnetic field is actively produced in electromagnets by applying energy from an external power source. In Lorentz force, the magnetic field will be considered present without any energy consumption in this comparison because of the use of permanent magnets. Some possible field sources are presented hereafter. Superconducting electromagnets are not considered since they need to be refrigerated, and they will consume more energy than non refrigerated electromagnets. The highest fields are reached in extremely short pulses (**?**). Nevertheless, those fields will neither be considered because will limit the possibilities of the actuation to very short periods of time. The strongest continuous man-made magnetic field is of 45 T (**?**). It is produced in a bitter electromagnet whose resistive part, which does not need superconducting refrigeration, produces 33.5 T. Nevertheless, bitter electromagnets have a high power consumption. This is because the magnetic field is generated in the air, which has low magnetic permeability (μ). The biggest forces cannot be reached by the highest power efficiency in electromagnets. If materials with higher magnetic permeability are used in electromagnets (e.g. iron) there is a saturation field above which any added power will not produce higher $\vec{B}$ fields. This behaviour is explained by a variable magnetic permeability with $\vec{H}$ field in ferromagnetic materials (**?**). Therefore, high permeability materials set a superior limit to the B value. Nevertheless, as energetic efficiency is being compared, fields produced in those materials are going to be considered, being the most efficient way to activate a $\vec{B}$ field.

To compare the energy consumption of Lorentz and magnetic forces, it is assumed that the electric current flows in the same conductor so resistivity will be the same in both phenomena. Therefore, the energy consumption comparison is equivalent to the electric current comparison. The magnetic force between two magnetic field sources is maximum when they are placed together. Assuming that they are equal electromagnets with the same $\vec{B}$, the total force for both magnetized surfaces obtained using the Maxwell stress tensor, is defined by Equation 1.3.

$$F = \frac{B^2 A}{\mu_0} \; [N] \tag{1.3}$$

where A is the area of each surface and μ_0 is the permeability of space. To maximize the force and minimize the consumption, the surface of the electromagnets placed together must be a circle. This is because the maximum possible area of a perimeter l is gotten from a circle of area $A = \frac{l}{2\pi}^2$ and minimizing the perimeter minimize the resistivity and thus the consumption. It is important to point out that the force decreases at least proportionally to the square of the distance between the electromagnets.

Furthermore, the current needed to generate the B value in an electromagnet, obtained using Biot-Savart law, is defined in Equation 1.4.

$$B = \mu n I \; [T] \tag{1.4}$$

where n is the density of turns per length of the conductor and I the electric current through that conductor.

As aforementioned, higher permeability materials produce $\vec{B}$ fields with less energy consumption. Therefore, Metglas 2714A (see appendix C) is chosen as the material looped with the electric current to generate the $\vec{B}$ field. It is the most efficient way to produce a magnetic field because it has the highest magnetic permeability $\mu_C = 1.256 \; \frac{H}{m}$ (**?**), which sets a superior limit in power efficiency. Nevertheless, Metglas 2714A has a saturation induction of $B_C = 0.57 \; T$. Therefore, the maximum force obtained at the maximum energy efficientcy is:

$$F_C = \frac{B_C^2 l^2}{4\pi\mu_0} = 20574.532 \; l^2 [N] \tag{1.5}$$

Taking that into account, the necessary current I to produce the maximum B value by means of two coils of $n = 1$ with magnetic permeability of Metglas 2714A is $I = 2\frac{B_C}{\mu_C} = 0.907A$.

In permanent magnet configurations, highest $\vec{B}$ fields are reached in Halbach configurations. These configurations consist of a rotation of the magnetization of a material along a path or a surface. This rotation, if correctly defined, augments the B value on one side while practically cancelling the field to near zero on the other side. If the rotation is made along a straight line, the configuration is called Halbach array (shown in Figure 1.1). When the rotation is done along a circumference, the resulting configuration is called Halbach cylinder (shown in Figure 1.2). Lastly, if this Halbach cylinder magnetization is generalized as the meridians of a sphere the resulting configuration is called Halbach sphere.

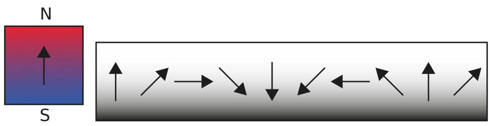

Figure 1.1: Magnetization pattern in a Halbach Array.

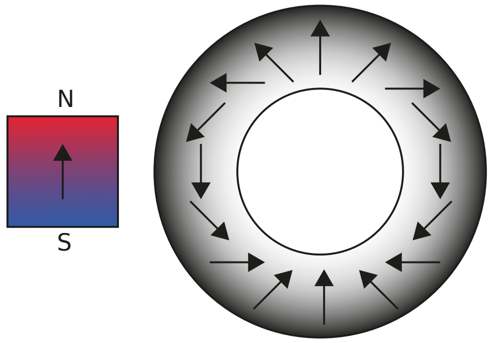

Figure 1.2: Magnetization pattern in a Halbach Cylinder.

Higher B values $B_X = 5\ T$ (**?**) are obtained in Halbach spheres configurations. However, these configurations are not easy to make. Therefore, the analysis carried out is done with a Halbach cylinder, which can easily provide fields of $B_Y = 1\ T$.

The force produced in an actuator by the Lorentz force is calculated by Equation 1.2. Considering the same length of the wire (l), as the perimeter of the current loop of an electromagnet, the same I and a magnetic field B_Y, the force is:

$$F_Y = B_Y\ I\ l = 0.907\ l\ [N] \tag{1.6}$$

Therefore, at equal power consumption, the force between two electromagnets is always lower if $20574.532\ l^2 < 0.907\ l$, which means sizes of:

$$l < 4.408\ 10^{-5}\ m \tag{1.7}$$

That result sets a point in length from which Lorentz force based actuators are always more energetically efficient than usual electromagnets devices.

With this limit, building actuators that surpass the energy efficiency of Metglas 2741A looks discouraging. However, if the technology is able to get those small sizes, some configurations explained in the following sections can be used to overcome those small sizes. It is important to notice that if the actuator moves through a path, which is essential to develop a work, the force of electromagnets will decrease at least with the square of the distance between the electromagnets. This is not the case in Lorentz force based actuators which force is constant through a path contained in a Halbach cylinder.

1.4 Modelling a linear Lorentzito

A first device, consisting of two copper wires with parallel currents, was tested. However, the mechanical resistance to deformation of copper made the Lorentz force approach useless. Geometries which multiply the force between wires, like springs, resulted in higher resistance to the material deformation. Moreover, high consumption and temperatures in wires were reached, getting even less force than in commercial solenoid valves dismissed as explained in Section 1.1. Therefore, the solely usage of wires and electricity seems a useless way to produce force and motion from Lorentz force. This test pointed out that the magnetic field $\vec{B}$ must be amplified to get higher forces with less consumption and heating. Furthermore, every mechanical deformation worsens the device performance, so they have to be avoided. These preliminary tests lead to a concept of an actuator consisting of a high $\vec{B}$ field area (to maximize Lorentz force) in which a single and not bendable conductor (to avoid mechanical losses) carries a current and is moved according to the Lorentz force. This force pulls linearly the conductor, which can be attached to any element to transmit the force. Because of its similarities to a cell and the Lorentz force usage, linear **Lorentzito** is proposed as its name, and will be used from now on in this thesis.

1.4.1 Nerve-cell-tendon model

Motion in actuators works and can be understood by the following process: by applying energy, a low potential energy space is set. Therefore, a free moving part affected by that potential is displaced to that space, generating motion. Generally, the moving part affected by the change of the potential is different from the part that gets energy to create that low potential space condition, as in electric induction motors or solenoid valves. In a Lorentzito, the simplest solution is an electrical wire which can act as the source of potential change and the source of movement. Therefore, all the elements attached to the wire move unless a variation is made to the actuator. That variation must be done because dragging any element connected to the conductor is an obstacle to get the maximum work of the actuator. The scheme proposed in Figure 1.3, which avoids this obstacle by separating the moving part from the potential generator part, is biologically inspired by myocites: it is similar to a nerve-cell-tendon block. In that block, the nerve is what transmits the signal that generates the low potential energy condition. The cell is what moves and the tendon is what transmits the motion. Therefore, the nerve is electrically connected to the cell and electrically isolated from the tendon. The cell is mechanically attached to the tendon and mechanically isolated from the nerve.

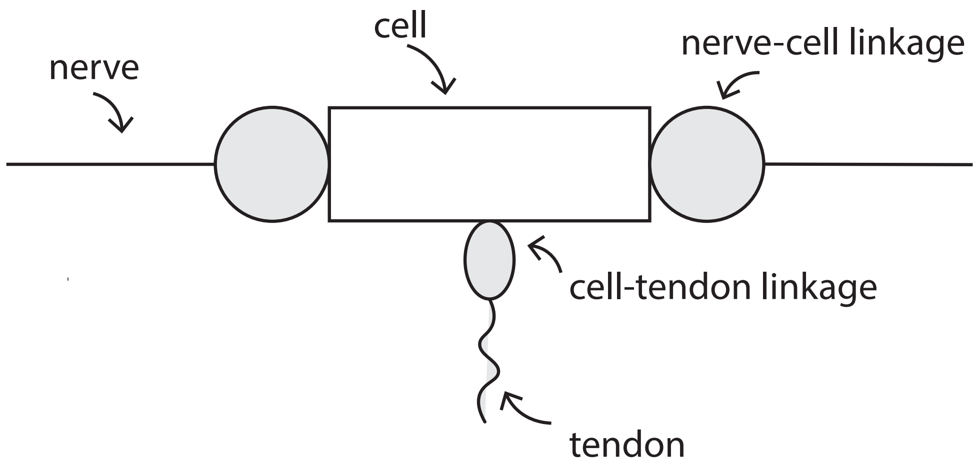

Figure 1.3: Nerve-cell-tendon model.

Any mechanical resistance or elasticity in the cell-tendon junction will decrease the final force transmitted to the tendon. That will be measured as the stretch ratio λ_t of the tendon's material (see Equation 1.8). Therefore, the non-ideal behaviour of nerve-tendon connection is represented by λ_t.

$$\lambda_t = \frac{l_t}{l_{wt}} > 1 \tag{1.8}$$

where l_t is the length of the tendon when a force generates a mechanical tension on it and l_{wt} is the lenght of the tendon when no force is applied to the tendon.

In terms of electricity, any conductor with higher resistivity than the movable part will consume more energy to generate the same force, resulting in a worse performance. Moreover, the nerve should be mechanically isolated from the cell-tendon sub-block, which has to be firmly connected, so it does not hinder the motion. The non-ideal behaviour of the the nerve-cell connection is modelled by the nerve-cell friction coefficient $\nu_{n-c} > 0$. An ideal nerve-cell-tendon implementation has $\lambda_t = 1$ and $\nu_{n-c} = 0$

1.4.2 The linkage problem

Attaching two pieces rigidly, as needed in the cell-tendon sub-block, is an easy problem. However, connecting two pieces electrically allowing a free and independent movement is not a simple task if the cell-tendon sub-block must be kept rigidly attached. This problem is named as the linkage problem. Therefore, a linkage problem appears in the junction between the artificial nerve and the cell. To partially or fully avoid the transmission of movement from the cell to the nerve, current must be transmitted without a rigid joint. An electric connection through a gas, plasma or liquid conductor with low friction between the non attached conductors could be used. Nonetheless, elastic conductors which provide low friction and stiffness could also be used. These four different joints between the nerve and the cell define a classification for Lorentzito: solid , liquid, gas and plasma nerve-cell connection. In this thesis only the liquid electrical connection will be analysed.

1.4.3 Electrical liquid connection

In a liquid electrical nerve-cell connection, as shown in Figure 1.4, electricity is transmitted through a liquid electrical conductor. Using that liquid as a joint provides very low friction and high conductivity. To avoid corrosion of salt solutions in conductors, metal alloys with low fusion point temperatures are the best option. Moreover, it is important to notice that any water-based solution could produce gases because of electrolysis, which is an undesirable effect. Nevertheless, liquid metals could be corrosive or toxic, and it should be taken into account for the selection of materials and shields to avoid deterioration and liquid leakages. Furthermore, a sealed region is mandatory in order to confine the liquid. This region will be the main source of ν_{n-c}. This electrical connection is the one proposed in this thesis for the Lorentzito actuator.

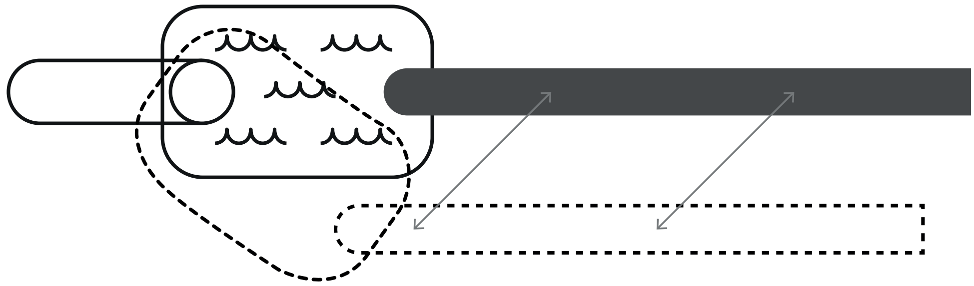

Figure 1.4: Depiction of a liquid electrical connection based on liquid joint.

1.4.4 Cell-tissue-muscle model

By clustering Lorentzito in series and parallel, as if they were cells of a muscle, a bigger linear actuator can be precisely designed. A scheme and explanation of this configuration will be shown in Section 2.7. If those actuators are considered as tissues, then some of them can be arranged as muscles in order to perform complex movements. Therefore, a set of simple linear actuators can accomplish very complex movements, such as those present in the human body or animals. That is the ultimate goal of designing this actuator. Nevertheless, reaching that goal is out of the scope of this thesis.

1.5 Document layout

In the next chapters, two structures based on models proposed in this thesis are going to be described. These structures involve geometry and materials decisions that will be covered in Chapter 2. Later on, a quick overview about configurations involving several actuators will be done.

In Chapter 3, different figures of merit will be proposed to measure and compare future implementations of Lorentzito. These figures of merit will be functions of the electric current and the size of the actuator. Then, the structures proposed in Chapter 2 will be simulated to calculate a theoretical superior limit to the figures of merit providing a design criteria. Those tables will define an electric current and a size to get a certain value in figure of merit.

In Chapter 4, the two defined structures will be implemented and tested. Its behaviour and design will be calculated and compared to the theoretical superior limit.

In Chapter 5, conclusions about the usage of the Lorentz force in the proposed models, structures and tests will be presented. Finally, some research lines will be proposed as future work to improve the understanding of Lorentzito actuators and its behaviour.

Chapter 2

Structure and materials

2.1 Description of a single actuator

A linear Lorentzito can be designed and built in many different ways by choosing different materials and geometries. The aim of this thesis is to design and test Lorentzitos as an alternative solution to commercial linear actuators in mimicking natural contractive movements and to implement the concept in a prototype. Therefore, not the best theoretical possible linear implementation is described, although some suggestions are going to be made. On the contrary, low cost and simplicity are more important for this first stage.

The proposed structure will be called **Parallelepiped Linear Lorentzito** because it resembles a composition of parallelepipeds. It consists of a magnetic structure to generate the $\vec{B}$ field, an inner conductor to carry an $\vec{I}$ perpendicular to the magnetic field, a tendon to transmit the movement, a region that solves the linkage problem and a case which contains all that elements. Two different structures shown in Figure 2.1a and Figure 2.1b will be presented.

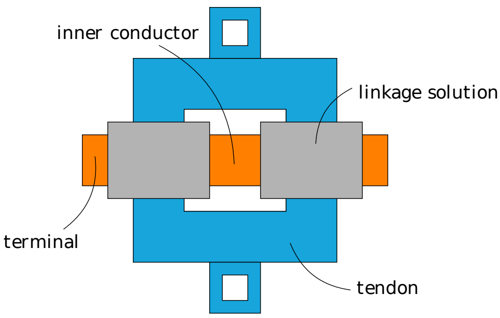

(a)

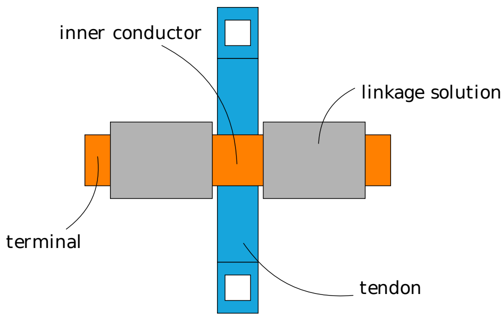

(b)

Figure 2.1: (a) Structure A and (b) structure B of the linkage solution.

The only difference between both structures is where the tendon is attached to the inner conductor. In Figure 2.1a the tendon is attached to two points leaving a space for the magnetic structure in the centre (not represented in the Figure). On the other hand, the structure shown in Figure 2.1b is only attached to one point. The motion has to be transmitted to the tendon from the centre of gravity of the inner conductor to avoid angular momentum since a linear Lorentzito is being designed. This implies that the magnetic structure needs a hole through which tendon will move.

2.2 Magnetic structure

The magnetic structure will generate the higher possible $\vec{B}$ field in a direction as perpendicular as possible to the current $\vec{I}$ flowing through the inner conductor.

The wire carrying current density will be considered rigid and will only be allowed to move in one dimension. Therefore, the $\vec{B}$ field has to be a constant vector field in order to generate a force that varies linearly with the current. In order to choose the magnetic configuration, cost, inner B value and mass are considered the most important parameters to optimize. Low cost is important because resources for this thesis are limited. Inner B value have to be as high as possible to ease the observation and measure of the Lorentz force in the actuator. Mass is important since this actuator is meant to imitate a muscle and useful muscles must develop enough force to lift themselves. Therefore, the lighter the Lorentzito the easier it will be to implement an artificial muscle.

To sum up, high $\vec{B}$ field and low mass cheap structures are sought. These characteristics can be obtained by a Halbach cylinder configuration (**?**). A Halbach cylinder is a hollow cylinder made of oriented magnetization pattern, defined by Equation 2.1, whose coordinates are defined in Figure 2.2a.

$$\vec{M} = M_r[cos((k-1)(\phi - \frac{\pi}{2}))\hat{\rho} + sin((k-1)(\phi - \frac{\pi}{2}))\hat{\phi}] \tag{2.1}$$

A uniform inner field is given when $k = 2$, that sets an inner field defined by Equation 2.2.

$$\vec{H} = M_r ln(\frac{R2}{R1})\hat{y} \tag{2.2}$$

Those configurations can also grant a small value of B outside a certain region enhancing the magnetic isolation between actuators which is relevant if placed together. It is important to poit out that, given a non infinite length, Halbach cylinders are affected by end effects which will curve the inner field at the base of the cylinder.

Halbach spheres are the three dimension generalization of Halbach cylinders. Its inner field given by $k = 2$ is defined by Equation 2.3. Being closed structures, there aren not end effects in Halbach spheres.

$$\vec{H} = \frac{4}{3} M_r ln(\frac{R2}{R1})\hat{y} \tag{2.3}$$

Although spheres can get higher and more uniform fields, they are more difficult to build and leave less space to its bore. Therefore, a Halbach cylinder will be used as the magnetic structure.

Halbach cylinders are a theoretical differential configuration that has to be approximated in a definite number of segments (?). Circular segments are more expensive than cubic magnets, so cubic magnets have been chosen to approximate the Halbach cylinder. Furthermore, they are easily stackable at four different magnetic orientation. The approximation of the Halbach cylinder made of cubic magnets is shown in Figure 2.2b.

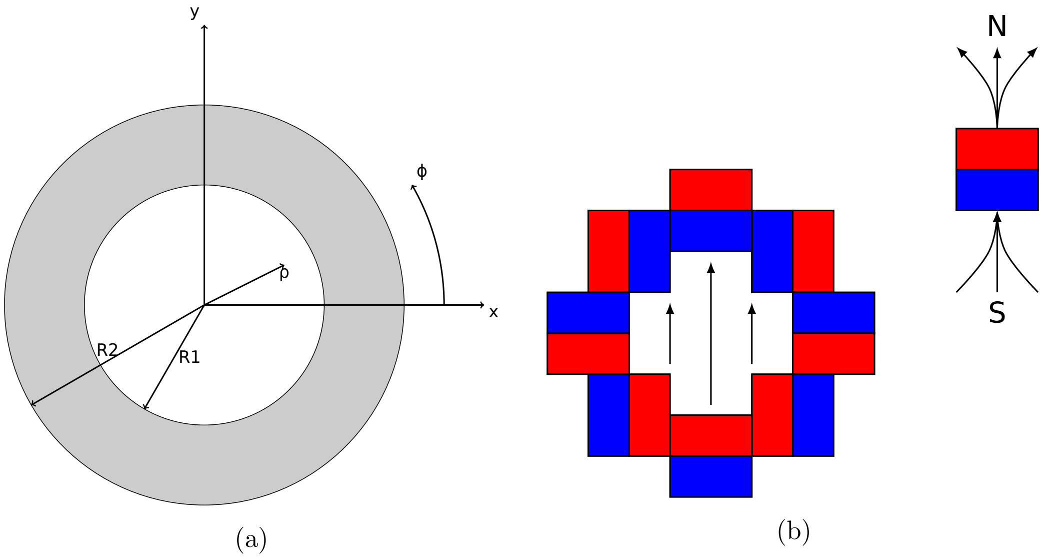

Figure 2.2: (a) Theoretical implementation and (b) aproximaiton made of cubic.

Amongst permanent magnets, NdFeB generates the strongest magnetic fields in the smallest size and weight commercially available (?). Therefore, NdFeB are going to be used. They are fragile and have a lower Curie temperature than other types of permanent magnets (?). That means that they can be demagnetize at lower temperatures than other material. Nevertheless, those temperatures are around 353 K, high enough for this application. Moreover, the magnets fragility is not relevant since they are going to be in a case which protect them tightly.

2.3 Inner conductor

The inner conductor is the part which carries the electrons. The current (I) that passes through a conductor depends on the electric resistance (R) of the wire. A low resistance means also that less power (P) is needed to get the same force, shown in Equation 2.4.

$$P = \frac{I^2}{R} \tag{2.4}$$

The resistance value is defined by Equation 2.5.

$$R = \frac{l}{A\sigma} \tag{2.5}$$

where σ is the electrical conductivity $[\Omega^{-1}m^{-1}]$, l is the length $[m]$ of the current path through the conductor and A is the cross-sectional area $[m^2]$ of the conductor through that path. If a more detailed analysis is needed, it is important to notice that σ is a temperature dependant parameter.

It is clear that big areas are desirable to decrease the resistance. That means that the maximum area should be covered by the conductor movement. The magnetic structure (see Figure 2.2b) leaves a prism whose base is a cross as a bore. Therefore, the maximum possible area covered in rectilinear displacement is obtained by another prism that fits in one arm of the cross.

The length is also related to the electric resistance and the power consumption. As length grows, electric resistance and power consumption grow too. On the other hand, the longer the conductor the bigger the force on it, considering that the conductor is in the $\vec{B}$ field. Both, resistance and force, depend linearly on the length, as shown on Equation 1.1 and Equation 2.5. Nevertheless, if the conductor height is greater than the magnetic structure's height, the $\vec{B}$ field will be smaller at sides and less orthogonal to electric current. That will produce less force in volumes where the resistivity is the same.

In conclusion, the best inner conductor shape, given the previous magnetic configuration (see Figure 2.2b), is a prism whose base is a square and its height is the same as the magnetic structure. This configuration maximizes the possible displacement of the conductor minimizing its resistance. The conductor is represented in orange in Figure 2.1a and Figure 2.1b. Side conductors, painted in orange too, and inner conductors are the same piece.

The material chosen for the inner conductor is copper. It has a good electric and temperature conductivity and is easy to acquire and mould. However, it is a diamagnetic material which will decrease and alter the magnetic field through itself. Moreover, diamagnetic materials' magnetic permeability is less than air magnetic permeability, which could decrease the B value in its surroundings and hence, the Lorentz force value. In future versions, it would be advisable to test ferromagnetic o paramagnetic materials which will strengthen the magnetic field. Nevertheless, scattering effects on electrons spins in the electric current could cancel the enhacement.

2.3.1 Inner conductor configurations

The inner conductor is the source of motion, so different configurations on its geometry and number can modify the behaviour of the actuator. If only one conductor is placed in the inner cavity, the movement can be transmitted to n tendons in the same direction (if external mechanisms are not added). Therefore, the movement will be very similar to a solenoid valve. However, if two conductors are placed in the inner conductor space, two independent directions can be transmitted to tendons, allowing more complex behaviours such as contraction. Moreover, two conductors will attract or repel each other because of the $\vec{B}$ field produced by their currents which would add up to the force transmitted.

Another interesting option to analyse is the direction of movement. If two artificial nerves are linked to the inner conductor, only two direction of movement will be possible since electric current can only flow in two different directions along the same path. For each additional pair of nerves attached to the inner conductor, one possible direction of movement can be added. It is important to notice that those directions will always share a plane. That is because the $\vec{B}$ field is assumed constant in direction and the cross product of the Lorentz force only allows movements perpendicular to that direction, which defines a perpendicular plane to $\vec{B}$ direction. That means that no matters which is the electric current direction, if $\vec{B}$ field is fixed, the Lorentz forces will always be contained in a plane. Therefore, for a linear actuator, there is no sense in building a Lorentzito with more than two artificial nerves, since only two directions are needed. For a planar actuator, three artificial nerves will be needed. That is because a set of two linearly independent vectors is basis to a plane ($\mathbb{R}^2$) and three points are needed at least to define two linearly independent vectors. Moreover, if $\vec{B}$ field is not considered constant in direction, a spacial Lorentzito can be designed with movements in three dimensions.

2.4 Tendon

The tendon, which transmits the Lorentz force, must be attached to the inner conductor, which is the source of motion. It has also to be accessible from the exterior of the actuator and rigid enough to avoid mechanical losses by deformation 1.8. Its shape has to be adapted to what the Lorentzito is attached to. Nevertheless, in this thesis a generic shape will be proposed with no specific purpose, so only rigidity and accessibility will be covered.

Lorentz force allows a linear movement in two possible directions. If only one tendon is placed at one side of the actuator, each direction of movement will be associated with a push or a pull movement. Therefore, to transmit pull and push movements, no matter the side the tendon is placed to, two tendons are necessary. To simplify it, both tendons will be implemented in one single piece, as shown in Figure 2.1 in blue. The tendon could be partially in contact with the linkage solution and the inner conductor. Nevertheless, as described in the linkage problem, it has to be mechanically isolated from the electric terminals. The material chosen is PLA because it is easy to print in three dimension printers and is rigid enough.

2.5 A linkage solution

To solve the linkage problem defined before 1.4.2, a solution based in liquid conductors is proposed. Metals, which are the better electric conductors, generally melt at high temperatures. Reaching high temperatures may often require an undesirable additional energy consumption. Nevertheless, some metals and eutectic alloys reach liquid state at low enough temperatures. Among them, some are toxic for humans like mercury and others are very reactive, like NaK alloy. From the most stable and safe for human health, an eutectic alloy called galinstan (**?**) has been chosen. It is made of gallium, indium and tin. Its melting point is 254.15 K and its boiling point is above 1573.15 K. It is a wide enough temperature interval to enable electrical connection through a liquid in many different situations.

The liquid in the linkage solution must be confined in a sealed defined region to avoid leakages. One end point of each rigid terminal of the actuator and the end points of the inner conductor must coexist in that region to allow the electric current transmission. The tendon can be partially submerged in the liquid metal as in Figure 2.1a or isolated from it as in Figure 2.1b. If it is partially submerged, the confinement must be elastic enough to allow the tendon movement without restriction. That will be accomplished with elastic membranes. These membranes will be the interface between the liquid and the air through the tendon. The design of those membranes' shapes is not trivial.

To understand the problem of designing these membranes, two types of transformation of a three dimensional surface will be defined. The first one is a stretch transformation in which two infinitesimal points change distance from each other, defining that distance as the minimum length path through the surface. The second one is a rotative transformation in which the defined distance is constant, but the relative position in three dimensions to at least one point is changed.

If the membrane changes its shape only by a rotative transformation, no energy will be stored and consequently no energy lost, because of the elastic properties of the membrane. That problem is similar to those solved by the Nash embedding theorem (?). The surfaces derived from that kind of problems are out of the scope of this thesis. Therefore, an heuristic technique has been developed to avoid stretching transformations as much as possible. It consists of creating a plane membrane as thin as possible and then wrinkle it to a fixed smaller area, that allows pseudo-rotation transformations that only modify the wrinkles and that almost do not stretch the surface. The material chosen for this membranes is latex, being a very elastic material and easy to purchase.

2.6 Case

The case is where all previous described parts will be placed together. It will isolate as much as possible the moving parts to prevent its deterioration. It will also prevent the breakdown of the actuator, since it can restrict the motion of the tendon and the inner conductor in better ways than the magnetic structure, because the material chosen for its construction does not have the conditioning of other parts.

An stackable shape is mandatory for the case in order to allow the construction of a complex actuator from singles Lorentzitos. The material chosen for the Lorentzitos designed in this thesis is PLA. This is because it is easily printable in 3D printers and is rigid enough. Nevertheless, to avoid mechanical looses, the case needs an extremely low friction coefficient so other materials such as PTFE or BAM should be tested in future implementations.

The case will also fix a position to the terminals. If no additional structure is placed or anything else is specified, the free movement of the inner conductor could lead it to get stuck with the terminals. This stuck can be avoided by physical walls. Nevertheless, if wire like solutions are implemented to connect electrically the inner conductor and the terminals in a linkage solution, some considerations must be taken into account. These stucks are prone to happen in solutions where the inner conductor can freely move in its longitudinal direction. An analysis is described then to avoid the stuck.

2.6.1 Analysis on distances on a liquid electrical connection Lorentzito

In this section, the location of the rigid terminals of the component, regarding the centre of the membrane, is analysed. This analysis is only relevant in implementations whose inner conductor can move freely in its longitudinal direction. To define the problem, the elements present in the the nerve-cell-tendon model in Figure 1.3 are simplified in Figure 2.3. In this figure, the green circles represent the electric terminals, the brown line represents the walls of the bore of the magnetic structure and the blue box represents the inner conductor. The linkages are not represented since they are considered variable. Black arrows point the direction of movement of the inner conductor and the yellow arrow points the direction of the current. The distances between relevant elements for this analysis are visually defined in Figure 2.4. Although Lorentzito needs two electric terminals, only one terminal is shown to simplify the figure. The hidden terminal is placed at the same distances.

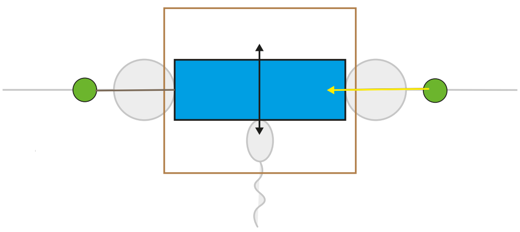

Figure 2.3: Geometric abstraction of the nerve-cell-tendon model to define distances in a liquid connection.

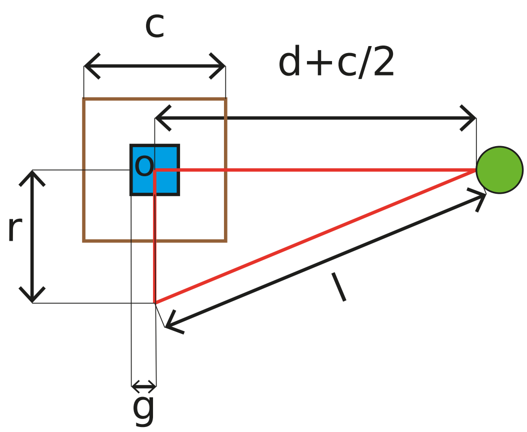

Figure 2.4: Graphic definition of the distances in a liquid connection.

O is the centre of the magnetic structure, c is the length of the magnetic structure in the direction of electric current, g is the distance between O and the end of the conductor in the direction of movement, $r-g$ is the maximum distance that the inner conductor can travel in the direction of movement from O, $\frac{c}{2}+d-g$ is the distance between O and the rigid terminals and l is the maximum length of a virtual line that connects the centre of the conductor and the centre of the rigid terminal of Lorentzito. This maximum length is gotten when $g=0$ as shown in Figure 2.4.

From this description, some conditions can be deduced that should be asserted to avoid stucks. In *Condition l*, shown in Equation 2.6, the minimum length of the electrical connection is defined by Pythagoras theorem in a right triangle.

$$l = \sqrt{(r-g)^2 + (\frac{c}{2} + d - \frac{g}{2})^2} \tag{2.6}$$

In that right triangle, one leg is the distance between a rigid terminal and the inner conductor $(r-g)$, when the centre of the inner conductor is placed at point O. This leg should be short in order to minimize the volume of the actuator. The other leg is the maximum distance the inner conductor can travel, $(\frac{c}{2}+d-\frac{g}{2})$. That movement is always perpendicular to the $\vec{B}$ field and the $\vec{I}$ current , which are fields with a constant direction, so it will follow a straight trajectory (shown as black arrows in Figure 2.3). This maximum movement sets the maximum distance that anything attached to the conductor can be moved. This sets, at a given current, the maximum amount of work and should be a design decision. Finally, l is the hypotenuse, so, as not to limit the maximum movement, this hypotenuse length must me reachable by the connection.

In *Condition d*, shown in Equation 2.7, the inequality must be verified to avoid the physical contact between the inner conductor and the rigid terminals.

$$d > \frac{l-c}{2} \tag{2.7}$$

Being l a possible length to the connection, the conductor can move horizontally in Figure 2.4, a distance equal to $l-(d+\frac{c}{2}-g)$. If this distance is greater than the separation between the inner conductor and the rigid terminals $d+\frac{c}{2}-g$, the conductor could touch them hindering the performance of the actuator.

In *Condition g*, shown in Equation 2.8, that inequality must be verified to ensure that the inner conductor is always in the constant $\vec{B}$ field region.

$$g < d + c - l \tag{2.8}$$

That means that it is always contained in the membrane. The conductor can move horizontally in Figure 2.4, an $l-(d+\frac{c}{2}-g)$ distance. If the centre of the conductor moves horizontally in Figure 2.4, more than $\frac{c}{2}-g$, a part of the conductor will be out of the constant $\vec{B}$ field region. The verification of Condition g is important in order to ensure a lineal response of the Lorentz force which ensures also a maximum response.

In *Condition k* , shown in Equation 2.9, k is the fraction of the inner conductor that can be outside the membrane when g, c, l and d are set.

$$k = 1 - \frac{l - d - \frac{c}{2} - \frac{c}{2}}{g} \tag{2.9}$$

This condition allows to set a limit to the minimum force that will pull the conductor considering that outside the membrane there is no magnetic field.

This four conditions have six variables, so there are two degrees of freedom. g and r are relevant in the power consumption and the maximum work of the actuator respectively. Hence, is advisable to fix g and r before the others. k is relevant to the linearity of the force behaviour so it should be fixed next, ideally to the value $k = 0$, which means a linear response. c is a parameter very important in order to let the component lift itself and in some performance ratios defined in Chapter 3. That means that c could be fixed by reasons alien to this four conditions. It is interesting to notice that only Condition l, shown in Equation 2.6, has the variable r and that the right triangle imposes three more conditions. The first one because the triangle inequality:

$$(r - g) + (\frac{c}{2} + d - \frac{g}{2}) > l \tag{2.10}$$

The other two because the hypotenuse is always greater than any of the legs:

$$l - (r - g) > 0 \tag{2.11}$$

$$l - (\frac{c}{2} + d - \frac{g}{2}) > 0 \tag{2.12}$$

2.7 Multiple actuators configurations

The Lorentzito actuator is proved to be better at small sizes compared to electromagnets (see Section 1.3). Nevertheless, minimizing the actuator's size will minimize the stroke too. Therefore, good figures of merit would be obtained for small sizes and very low range movements for each actuator. This movements could be too small to do many useful tasks that other linear actuators are able to accomplish. In order to extend the advantages of small actuators in wider ranges of movement, multiple linear Lorentzito must be attached.

If the purpose is to get longer paths of movement, every artificial tendon can be attached to another Lorentzito, creating a serial configuration as seen in Figure 2.5. This will only be useful if every Lorenzito is able to lift the next Lorentzito to which it is attached. If every Lorentzito in the configuration weights the same, the previous assumption means that $\rho_m > 1$, a figure of merit which will be defined in Chapter 3. The length can be controlled easily by the number of Lorentzito activated and, therefore, the maximum work will be bigger than in a single Lorentzito.

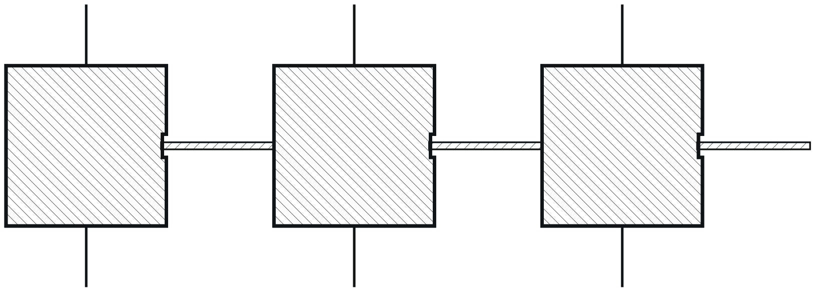

Figure 2.5: Serie Lorentzitos configuration.

Placing Lorentzito in series will not strength the final force. At the end of the configuration, the force will be the same as if only one Lorentzito would be pulling. So in order to increase the final force, the artificial tendons can be attached in parallel as shown in Figure 2.6.

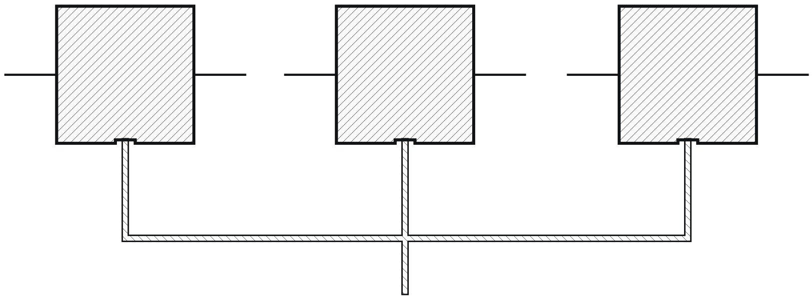

Figure 2.6: Parallel Lorentzitos configuration.

Those configurations allow to increase the work increasing the maximum force or the maximum displacement.

Chapter 3

Simulation

In this chapter figures of merit will be defined to evaluate the actuators behaviour. Before designing the actuator, some parameters are going to be simulated to test the magnetic structure and materials chosen. This simulated parameters will be used to calculate theoric figures of merit and to set a superior limit to the performance of a Parallelepiped Linear Lorentzito.

3.1 Figures of merit

In order to evaluate the design of a linear Lorentzito, some parameters are defined. This parameters will define figures of merit to compare the actuator performance with other actuators, allowing to place Lorentzitos in a context and to compare different implementations. A force-consumption rate, a mass ratio and a general rate are defined to accomplish that goal. In a Lorentzito, the only irreplaceable part is the conductor. Therefore, volume and mass efficiency quotients are defined to measure the use of structures different than the inner conductor.

In the figures of merit of the Parallelepiped Linear Lorentzito, some assumptions are made: the wire carrying current density is rigid, the $\vec{B}$ field is considered a constant vector field and the inner conductor is a cube of the same size as the cubic magnets in the magnetic structure. It is interesting to notice that in a cube, the volume equals to the cube's edge powered to three whereas its section area (parallel to one of its faces) equals the edge powered to two. That means that the conductor weight will grow faster with size than conductance, as conductance will grow faster with size than Lorentz force pulling that conductor. This is relevant in the useful size of linear Lorentzitos since force will be proportional to the edge, the power consumption to the edge powered to two and the weight of the inner conductor to the edge powered to three. This is important because in a Lorentzito actuator the force will always have to carry the inner conductor. This concept and other relevant conclusions will be translated in following described figures of merit.

3.1.1 Force-consumption quotient

The greater the force-consumption quotient ($\rho_{\frac{N}{W}}$), the greater the energy efficiency in generating the force, defined by Equation 3.1.

$$\rho_{\frac{N}{W}} = \frac{F}{I^2\ R} = \frac{B\ l^2}{I\sigma}\ [N/W = s/m] \tag{3.1}$$

where F is the value of the Lorentz force in the actuator, I is the electric current supplied to the actuator and R is the electric resistance of the actuator. The last expression is the result of expressing force (F) as the modulus of Equation 1.2 and expressing resistance (R) as in Equation 2.5.

3.1.2 Mass quotient

The greater the mass quotient (ρ_m), the greater the mass a Lorentzito can lift against gravity acceleration normalized by its own weight. $\rho_m < 1$ means that the actuator is not able to lift its own weight. $\rho_m > 1$ is mandatory for configurations explained in Section 2.7. This quotient is defined by Equation 3.2.

$$\rho_m = \frac{F}{g\ a_m} \tag{3.2}$$

where F is the value of the Lorentz force in the actuator, g is the gravitational acceleration and a_m is the mass of the actuator.

The minimum actuator mass is the inner conductor mass $a_m = l^3 c_D$ and Lorentz force is $F = BIl$. Therefore, $\frac{B\ I}{g\ l^2\ c_D}$ is the superior limit to this quotient, where B is the magnetic field value in the magnetic structure's bore, I is the electric current supplied to the actuator and c_D the mass density of the inner conductor. This superior limit represents the fact that at least the conductor, considered as a cube of edge l, is needed to generate force, so the minimum mass of the actuator is the mass of its electrical conductor.

3.1.3 Force-mass-consumption quotient

The force-mass-consumption quotient ρ, defined by Equation 3.3, is used to merge both previous quotients into one rate and to evaluate both conditions at a time. This is done by multiplying both normalized quotients: $\widetilde{\rho}_m\ \widetilde{\rho}_{\frac{N}{W}}$. Quotients are normalized in order to get a value which gives same weight to both parameters. ρ is calculated for an interval of currents (I) and an interval of sizes (l). The normalization is done by subtracting the minimum value of the quotient in these intervals and dividing the result by the difference between the maximum and minimum value of the quotient. To get an useful result the intervals must be the same for each quotient. It means $0 \leq \rho \leq 1$.

$$\rho = \widetilde{\rho}_m\ \widetilde{\rho}_{\frac{N}{W}}\ [N/W = s/m] \tag{3.3}$$

3.1.4 Volume efficiency coefficient

The minimum limit size of the actuator is given by the inner conductor. Therefore, an efficiency volume coefficient, defined by Equation 3.4, is defined to evaluate how close to that limit the component is. This limit is related to the mass of the actuator through the volumetric mass density of materials used in the design.

$$\epsilon_v = \frac{c_v}{a_v} \tag{3.4}$$

where c_v is the volume of the inner conductor and a_v is the volume of the actuator.

3.1.5 Mass efficiency coefficient

The lower limit for the mass of the actuator is given by the inner conductor. An efficiency mass coefficient is defined by Equation 3.5 to evaluate how close to that limit the component is. This limit is related to the volume of the actuator through the mass density of materials used in the design.

$$\epsilon_m = \frac{c_m}{a_m} \tag{3.5}$$

where c_m is the mass of the inner conductor and a_m is the mass of the actuator.

3.1.6 Maximum performance time

A steady operation of the component will be considered when a steady current flows through the inner conductor. That current will dissipate heat by Joule-Lenz law of heat dissipation, shown in Equation 3.6.

$$P \propto I^2 R \tag{3.6}$$

This heat will raise the temperature of the actuator demagnetizing the magnetic structure or melting some materials. Therefore, that heat will limit the maximum time the actuator can be in that steady operation. That time will be called maximum performance time (t_{max_i}) and will be proportional to the electric current flow, as showed in Equation 3.7.

$$t_{max\_i} \propto I_i \tag{3.7}$$

To avoid the demagnetization of the magnetic structure, heat dissipation has to be low enough to never reach the Curie temperature on permanent magnets. That is the temperature above which a magnets will lose their permanent magnetic field. Hence, there is a theoretical maximum work due to the Curie temperature which depends on the heat transfer in the electrical currents and its transmission to the permanent magnets. That theoretical maximum depends on the configuration and construction of the Lorentzito and will set a limit to the time a certain current can be supplied to the actuator and hence to the time a certain force can be sustained. Thermal isolation of magnets from heat sources and a good refrigeration will rise the performance of the actuator. If refrigeration is not good enough while electric current is flowing, the component will need to stop to refrigerate the magnets. That time, called maximum performance time (t_{max_i}), will be defined as the time in which Lorentzito magnets reach Curie temperature because of electrical heating of the conductors from a room temperature, 298.15 K, and an off state. That time will be proportional to the current applied, which will be determined by the ampacity of the conductors and ideally will tend to infinite.

3.1.7 Maximum current

The greater the electrical current the greater the temperature of the conductor. A rise of that temperature will decrease the electrical conductivity of the conductor. The inner conductor should be a solid, so temperatures above the melting point must be avoided. That puts a limit to the maximum electrical current. Considering that the melting point is never reached, another phenomenon put a limit to the current. That is the $\vec{B}$ field produced by the flowing current in the conductor determined by the Ampere law. This field can be high enough to demagnetize the permanent magnets nullifying any possible force due to the lack of magnetic field perpendicular to current. That field will be perpendicular to the current direction and depends a lot on the configuration of the actuator. A lateral magnetic shielding with high permeability could be used in order to protect the permanent field on magnets.

3.1.8 General considerations

To implement an optimal Lorentzito, some physical properties of the materials must be taken into account. All materials should have low density in order to increase the ρ_m ratio. Permanent magnets should have high remanence to increase $\vec{B}$ field and high enough coercivity to withstand adjacent magnets field and $\vec{B}$ field due to moving charges in the inner conductor. High enough Curie temperatures are needed also in order to increase t_{max_i}. The tendon should have a very low λ_t to transmit all the movement of the inner conductor to what is moved. Furthermore, the electrical conductivity of the conductor should be high and independent enough of the temperature to increase $t_{max\ i}$. Finally, inner conductors with high permeability could be used to amplify the inner $\vec{B}$ field which is the responsible of Lorentz force if scattering effects of spin electrons in the electric current are low enough.

3.2 $\vec{B}$ field in the magnetic structure

The differential equations in magnetic problems are complex so its solutions are approximated. A free software, called Agros2D (**?**), will be used to calculate and represent numerically the inner fields. Values of magnetic properties used in the simulations are described in table 3.1.

Table 3.1: Magnetic properties of materials in simulation.

$Material$	μ_r	$B_{rm}[T]$
Air	1	0
$Magnets$	1.07	1.1

The simulated $\vec{B}$ field will be generated by permanent magnets oriented as in a Halbach cylinder. A Halbach cylinder is a hollow cylinder with a certain oriented magnetization explained in Section 2.2. A section of this structure is a circular crown that has to be approximated by the square shape of cubic magnets as shown in Figure

2.2b. This configuration is simulated in Agros2D and the result of the simulation is shown in Figure 3.1.

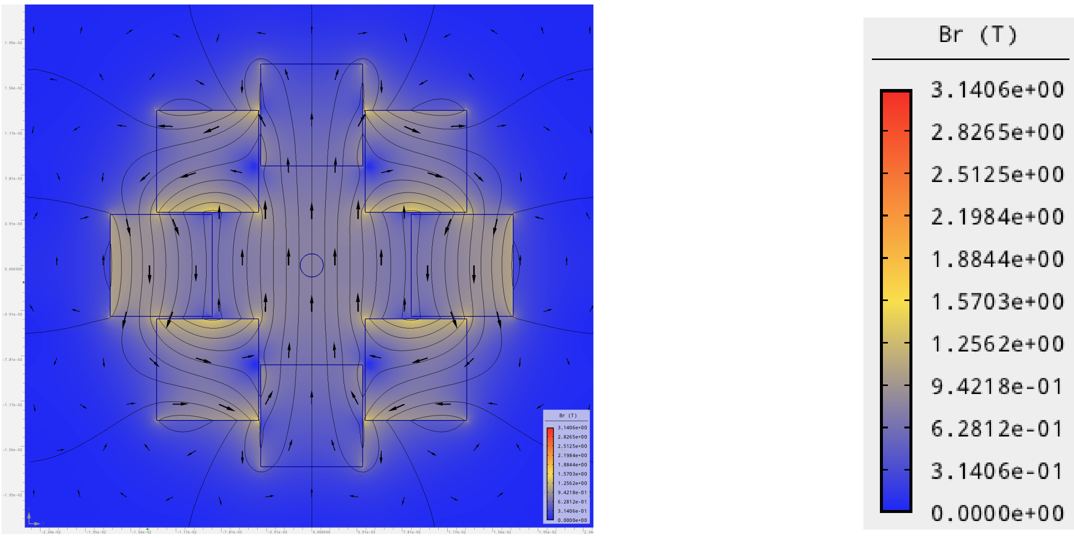

Figure 3.1: Magnetic field in the magnetic structure.

There are eight cubic magnets placed with their centre in a circumference as close as possible. That closeness avoids end effects between magnets. Iron could be placed inside the inner region in order to amplify the magnetic field and confine it, but it is not present to simplify the construction. The $\vec{B}$ field is not as constant as in ideal Halbach cylinders and presents some points of zero field. Nevertheless, this points are not in the trajectory of the inner conductor motion. It also has a deviation in $\vec{B}$ direction near cubic magnets. That deviation will decrease the Lorentz force since only $\vec{B}$ perpendicular to $\vec{I}$ generates that force. The B value across the inner conductor trajectory is shown Figure 3.2.

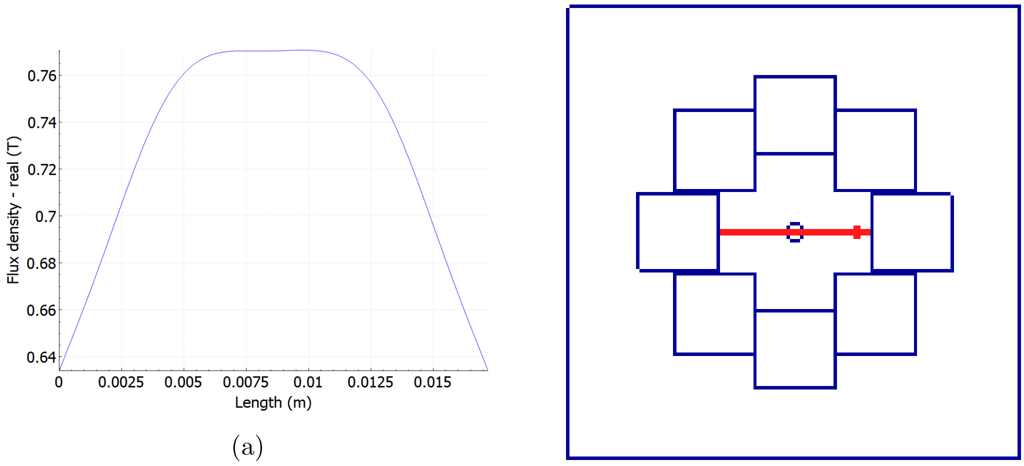

(a)

(b)

Figure 3.2: (a) Magnetic field value through the red line (b) in the approximation of a Halbach cylinder.

The B value of the magnetic field is noteworthy smaller near magnets and higher in the centre of the structure. Arithmetic mean of B along the inner conductor trajectory is 0.73 T. In the simulations carried out, scaling geometries do not change $\vec{B}$ field values. Therefore, it is assumed that scale is not relevant in the solutions. The theoretical formula of the inner field of a Halbach cylinder (see Equation 2.2), which only depends on the relation between its inner and outer radio, suggest the veracity of the results of the simulation.

3.3 Electrical conductor and connection

In the actuator, the electricity flows through solid and liquid materials. The solid materials are present at the electric terminals of the actuator, in the inner cavity of magnetic structure and in the tendon which is attached to the inner conductor. The liquid material is present between the solid conductors and may be in the inner cavity of the magnetic structure. The electric properties of the materials in the simulation are defined in Table 3.2.

Table 3.2: Electric properties of materials in simulation.

$Material$	σ
$GaInSn$	3.46×10^6
$Copper$	5.96×10^7
PLA	5.96×10^{-15}

The situation in which liquid and solid conductors share the $\vec{B}$ field region is simulated. It is the more interesting situation since if the liquid of the linkage solution does not goes into this region, it only acts as an electrical conductor and the behaviour of the inner conductor is not modified. Therefore, if the liquid conductor and the inner conductor share the constant $\vec{B}$ field region are simulated. As electric current flows trough both conductors but only the solid transmits the force out of the actuator some force will be lost. The solid should have a higher conductivity in order to gather more electric current than the liquid conductor.

In the simulation, currents are solved when there is an electric potential difference of 0.1 V between electric terminals. The structure simulated follows the structure represented in Figure 2.1a. The section in the plane of movement is represented in Figure 3.3.

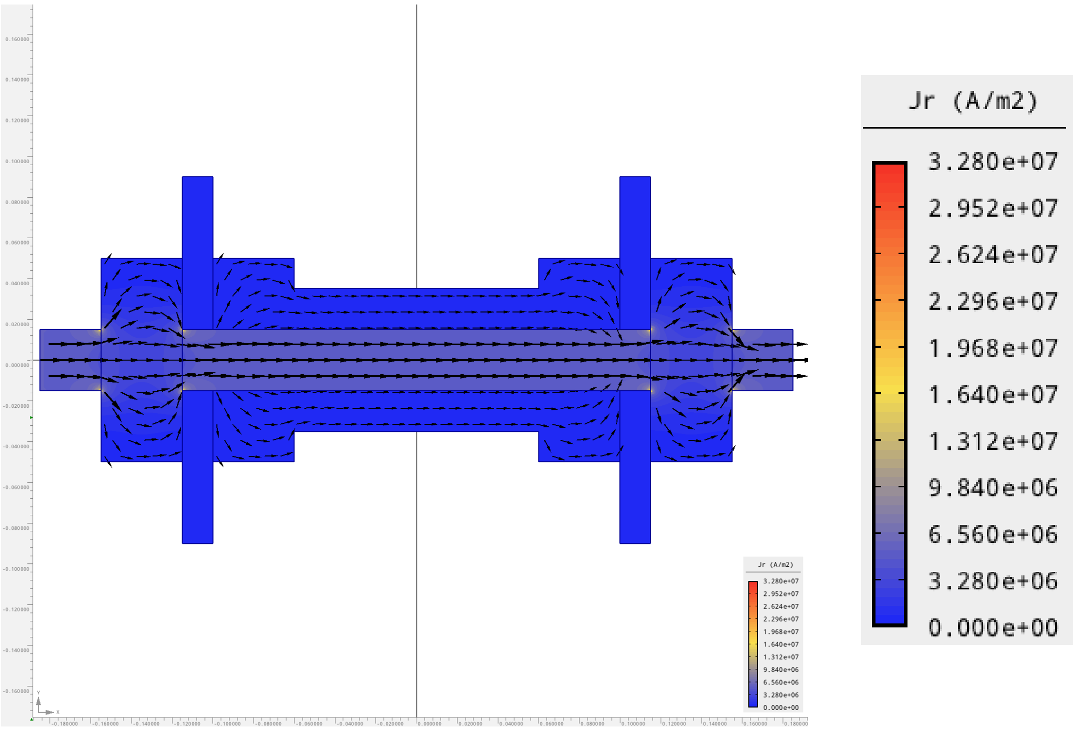

Figure 3.3: Electric currents in the plane of movement.

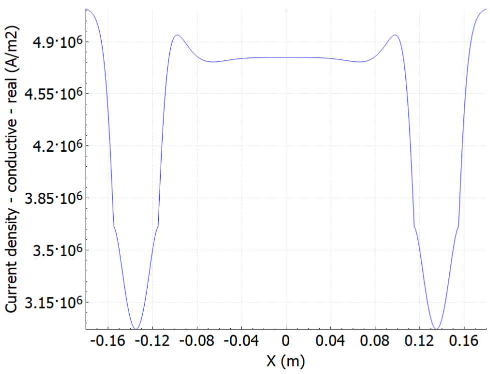

(a)

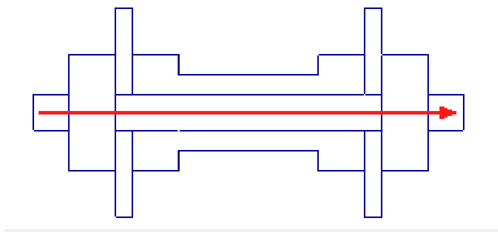

(b)

Figure 3.4: (a) Electric current density field value through the red line (b) in the electric terminals and inner conductor.

Figure 3.4a represents the value of the current density through the red path shown in Figure 3.4b. The direction of the electric current can be considered orthogonal to the $\vec{B}$ field in the inner cavity. Nevertheless, because of the small difference of conductivity between Galinstan and copper, a significant amount of current at terminals does not flow to the solid conductor and a percentage of current flows through Galinstan. This is an undesirable effect, because the liquid does not transmit its movement. Moreover, its movement generates a high and a low pressure area which hinders the copper movement. This is because direction of electric current calculated in Figure 3.3: if $\vec{B}$ goes inwards then copper goes up. Nevertheless, the Galinstan placed near the upper edges of the centre copper piece goes to the upper-centre of the figure. On the other hand, near the lower edges of the centre copper piece, Galinstan goes up and out of the centre. Different directions of movement produce a higher pressure in the upper region than in the lower region of the constant $\vec{B}$ field. Therefore, pressure is higher in the direction of movement and the force transmitted outside the actuator is weaker than the Lorentz force present in the copper.

To sum up, two reasons of force losses are found in the simulation. One is the short difference between copper and Galinstan conductivity. The other is the difference in pressure because of the electric current direction at the edges of the centre rigid conductor. It is interesting to notice that the size is not relevant since same configurations with different sizes does not change $\vec{J}$ field values.

3.4 Designing tables

Considering the magnetic and electric structures simulated, the theoretical figures of merit defined in Section 3.1 can be calculated. Size and electric current (I) are set as variables. The size in the proposed structures is proportional to the edge of cubic magnets (l). Therefore, the variable size will be represented by a variable l. It is assumed that the electric current follows a straight path perpendicular to $\vec{B}$ field. Additionally, it will be considered that only the 95% of the electric current contributes to the Lorentz force as simulations suggest when the liquid conductor is present. B

value is considered the mean value obtained in the simulation, $B = 0.73\ T$

This representation of figures of merit can be used in order to choose size and power supply given the structure, materials and geometry of a Parallelepiped Linear Lorentzito. It is assumed that the inner $\vec{B}$ field is constant at all scales of the configuration, which has been tested in simulations. In the following figures, only values of length l and current I which result on $\rho_m > 1$ are represented. That decision is done because only those values are interesting for Lorentzitos as explained in Section 2.7.

3.4.1 Superior limit of a Lorentzito

In order to set a limit to figures of merit, the structure analysed in this section has the essential materials and the quantity to make Lorentzito properly work. Those materials are NdFeB magnets which generate the magnetic field, Galinstan, that allows a free movement and Copper, that is moved by Lorentz force. Although in a real actuator are necessary, electric terminals and structural materials are not present in this analysis. So these figures of merit set a limit to prototypes and a framework to asses the quality of a prototype or an actuator.

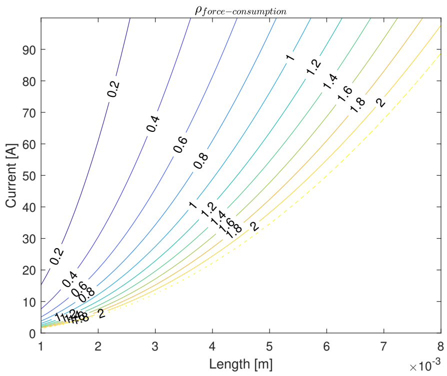

Figure 3.5: $\rho_{\frac{N}{W}}$ force-consumption quotient contour lines at intervals $I \in [0, 100]$ and $l \in [10^{-3}, 80^{-3}]$ for an ideal Lorentzito.

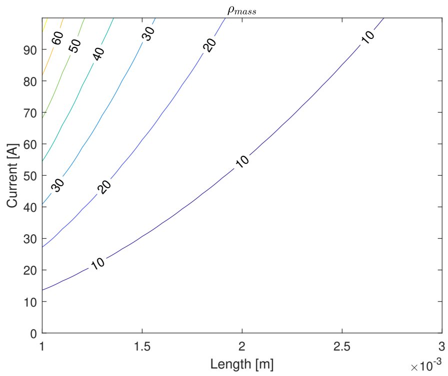

Figure 3.6: ρ_m mass quotient contour lines at intervals $I \in [0, 100]$ and $l \in [10^{-3}, 30^{-3}]$ for an ideal Lorentzito.

Figure 3.5 shows that bigger actuators have better energy efficiency $\rho_{\frac{N}{W}}$. This is because the energy stored in bigger magnets is in bigger volumes at equal energy density and because of the reduction of resistance due to resistivity dependence of the cross-sectional area shown in equation 2.5. However, Figure 3.6 shows that the little the better, in order to lift it's own mass against gravity.

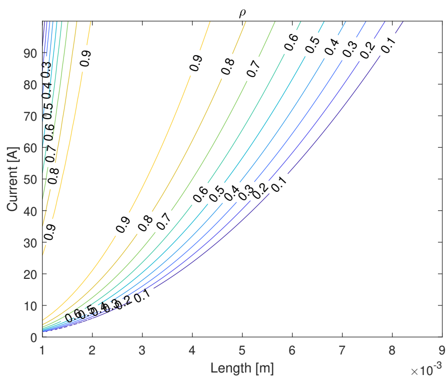

Figure 3.7: ρ force-mass-consumption quotient contour lines at intervals $I \in [0, 100]$ and $l \in [10^{-3}, 90^{-3}]$ for an ideal Lorentzito.

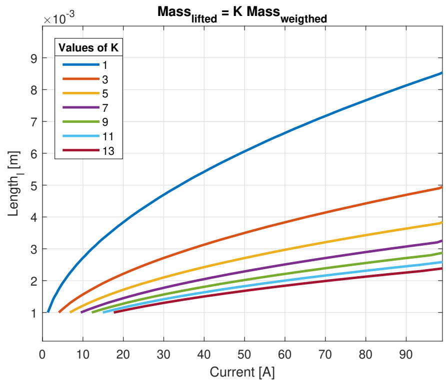

Figure 3.8: Times actuator mass that is lifted at intervals $I \in [0, 100]$ and $l \in [10^{-3}, 10^{-2}]$ for an ideal Lorentzito.

As two variables are desirable to be as big as possible, the ρ parameter in Figure 3.7, which evaluates both ρ_m and $\rho_{\frac{N}{W}}$ in one parameter, is calculated to take the best decision. In that graphic there is a clear region where Lorentzitos should be in order to optimize their behaviour.That is the region confined between the 0.9 contour lines which means high mass quotient at the same time as force-consumption quotient. Finally, Figure 3.8 shows how big must the component be in order to lift K times its own mass at a given current. This graphic shows that the reduction of size is more relevant at lower sizes. High K is desirable so the actuator should be minimize as much as possible until physic limitations are founded.

These figures do not only provide a superior limit to a Lorentzito performance but are also a tool to its design. They provide, for each structure and materials, information to take decisions in order to solve a specific problem with Lorentzitos.

Chapter 4

Implementation and tests

4.1 Implementation

In this section two different implementations are analysed. One is the implementation of the structure proposed in Figure 2.1a and the other is based on the structure proposed in Figure 2.1b. The ideas presented in the previous section inspire both but with two differences: where the tendon is placed and the shape of the linkage solution. In the first tests, equipment available is not able to supply electric currents higher than 7 A. Therefore, little sizes are desired to get high ρ values. However, minimum size reached in this thesis is that in whose magnets are cubes of three millimeter of edge.

4.1.1 First implementation

In the first implementation, the tendon is partially immerse in the liquid conductor and the linkage solution is a volume where tendon, inner conductor and electric terminals coexist. Its parts are hereafter presented and explained.

The magnetic structure, shown in Figure 4.1a, has been designed in Autodesk Inventor 2018 (**?**) and lately printed in a Hephestos 2 (**?**) using PLA filament. The magnets are cubic NdFeB magnets of 3×10^{-3} of edge and 1.1 T of remanence. The inner conductor is a block of polished copper that slides in the bore of the magnetic structure, shown in Figure 4.1b. It is placed in the bore of the magnetic structure. The linkage solution implemented is shown in Figure 2.1a. Two membranes of latex are created to allow the tendon movement in each one of the two possible directions. They have wrinkles that allow the movement without hinder too much the motion of the inner conductor. They are placed on top of a PLA structure that envelope the magnetic structure.

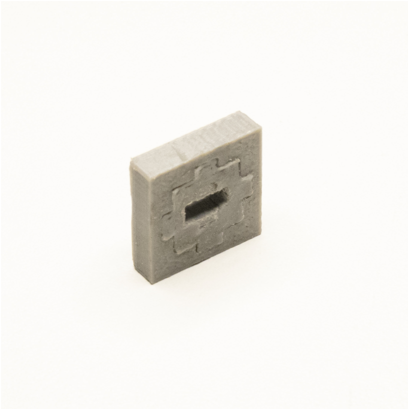

(a)

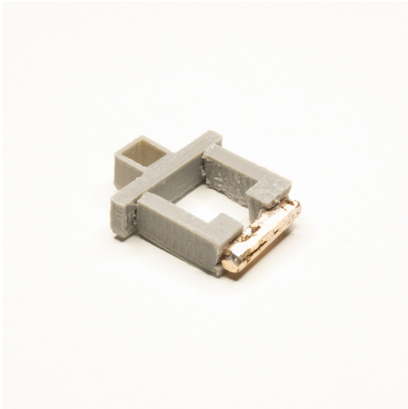

(b)

(c)

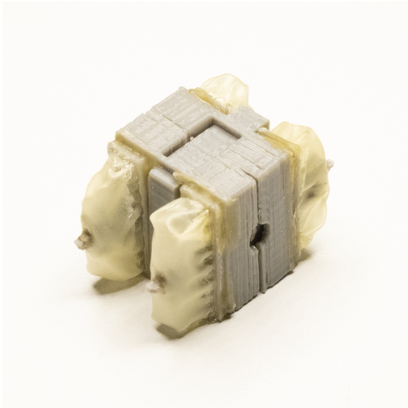

(d)

Figure 4.1: (a) Magnetic structure, (b) half of a tendon and the inner conductor, (c) linkage solution, (d) magnetic structure, tendons and inner conductor.

The tendons, made of PLA, hold the inner conductor as shown in Figure 4.1b. They are polished to avoid mechanical losses through friction. The tendons, the inner conductor and the magnets are placed together as shown in Figure 4.1d.

The actuator is assembled as shown in Figure 4.2a. The case, shown in Figure 4.2b, holds the actuator in place and allows the movement of the tendons and the inner conductor through a hole. It includes the electric terminals where power supply will be connected.

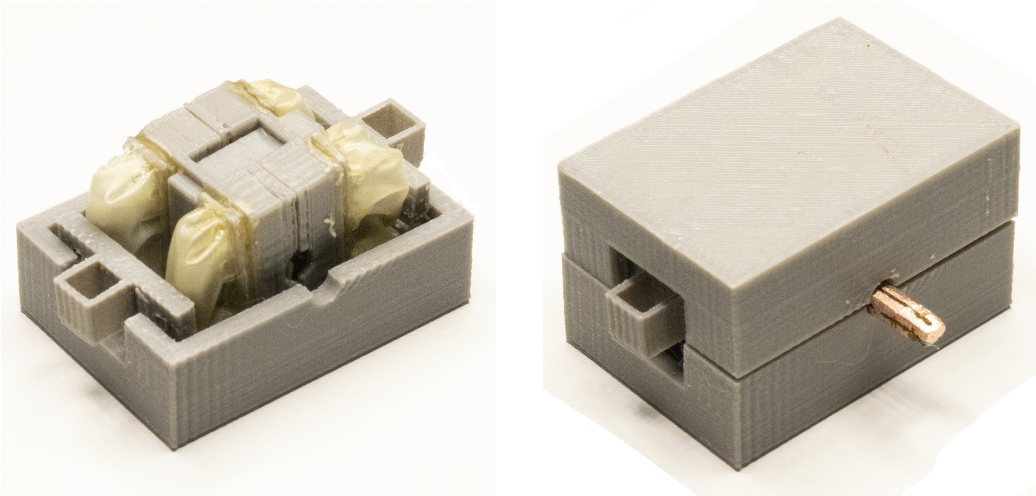

(a) (b)

Figure 4.2: (a) Linkage solution assembled and (b) Parallelepiped Lorentzito.

4.1.2 Second implementation

In the second implementation the tendon is not immersed in the liquid conductor and the linkage solution is a surface where only the inner conductor and the electric terminals coexist. As in the first implementation, all structural support has been designed in Autodesk Inventor and lately printed in a Hephestos 2 using PLA filament.

The inner conductor and the magnetic structure, shown respectively in Figure 4.3a and Figure 4.3b, are the same as for the first approximation. The tendon is shown in Figure 4.3c. It is connected to the inner conductor in its center.

(a) (b) (c)

Figure 4.3: (a) Inner conductor, (b) magnetic structure and (c) tendon.

The linkage solution implemented is shown in Figure 4.4a. The linkage solution followed is shown in Figure 2.1b. Two membranes of latex are created in a shape similar to a planar surface. These shapes present a very low resistance to bend over any axis contained in the plane and high resistance to bend over any axis not included in the plane. Those are placed in a way that the inner conductor motion will produce a bending over an axis contained in the plane to lower the interference to its motion.

(a)

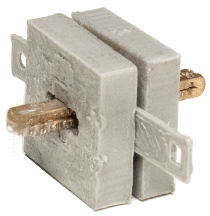

(b)

(c)

Figure 4.4: (a) Linkage solution, (b) assembly of inner conductor, magnetic structure and tendon and (c) case.

The tendon, made of PLA, holds the inner conductor between two magnetic rings as shown in Figure 4.4b. It is polished as the inner conductor to avoid mechanical losses through friction. The tendons, the inner conductor and the magnets are placed together as shown in Figure 4.4b. The case, shown in Figure 4.4c, holds the actuator in place and allows the movement of the tendons and the inner conductor through a hole.

4.2 Tests

The aim of these tests is to corroborate how good is the real implementation related to the ideal figures of merit. If good enough, they will also prove that Lorentzito is an alternative to existing technologies.

Firstly, it is necessary to know the magnetic field generated inside the magnetic structure. Instead of being measured, it is indirectly calculated as explained hereafter. A current is pumped with no load to test how much electric power is necessary to lift the inner conductor. As the inner conductor weight and length and the current are known, an effective B_e field is defined by Equation 4.1. This field is used to calculate the necessary current to lift a weight.

$$B_e = \frac{c_m}{I\ l}[N] \tag{4.1}$$

where c_m is the inner conductor mass, I is the electric current pumped and l the length of the inner conductor.

To set the maximum time of work, the Curie temperature of the permanent magnets or the burning temperature of the actuator will be considered. If Curie temperature is reached, the magnets will lose their magnetic field and the actuator will be considered broken. So the temperature of the core should be observed until it reaches that temperature at different currents and a current-time graphic will be defined. It is important to check after this experiment if the $\vec{B}$ fields generated by the inner conductor have demagnetize the magnetic structure. In that case, the maximum current will be defined as the maximum current that does not demagnetize the membrane.

The maximum continuous force then to be considered is the one obtained with the maximum current that never reaches the Curie temperature, burns the actuator or demagnetize the permanent magnets. That current will be named as the operation current (I_{op}) and will depend on the refrigeration of the conductor. By knowing the operation current, the effective field (B_e), the volume and the mass of all figure of merit will be defined. As I is the sole free parameter, all graphics figures of merit will be a function of it.

It is important to state that the maximum current discussed was never reached, because the power supplies available were not able to provide that current. Therefore, no analysis is done in this regard.

4.2.1 First implementation

The first implemented Lorentzito has a resistance of 0.01 Ω measured from electric terminals. Available power supplies provided a maximum of 7 A in this thesis. 7 A were not enough to oppose all the forces and to lift the inner conductor. Therefore, calculating the effective magnetic field was no possible. Some effects are proposed as reasons of those opposing forces:

- The elastic constant of the latex of membranes may be too high presenting a too high nerve-cell friction coefficient ν_{n-c}. Membranes also present friction forces in their wrinkles.

- Galinstan in the constant $\vec{B}$ field region behaves opposing the movement of the inner conductor as mentioned in Section 3.3. As it partially carries the electric current, Lorentz force also pulls it in the direction of movement. That generates high pressures in the direction of movement and low pressures in the opposite direction that hinder the inner conductor motion.

Figures of merit were not calculated since no force could be measured. Compositions of more than one Lorentzito where neither tested because the available electric current was not enough to lift the inner conductor. Nonetheless, tests did not produce demagnetization of the magnetic structure or burning in the implementation.

4.2.2 Second implementation

The tests of the second implementation are made on the structure shown in Figure 4.5. The actuator has to lift a known weight (blue in Figure 4.5) against gravity. Current and voltage are measured with a multimeter independent from the power supply and force is calculated from the weight lifted. Only currents of $7A$ were tested, because lower currents are not significant in behaviour.

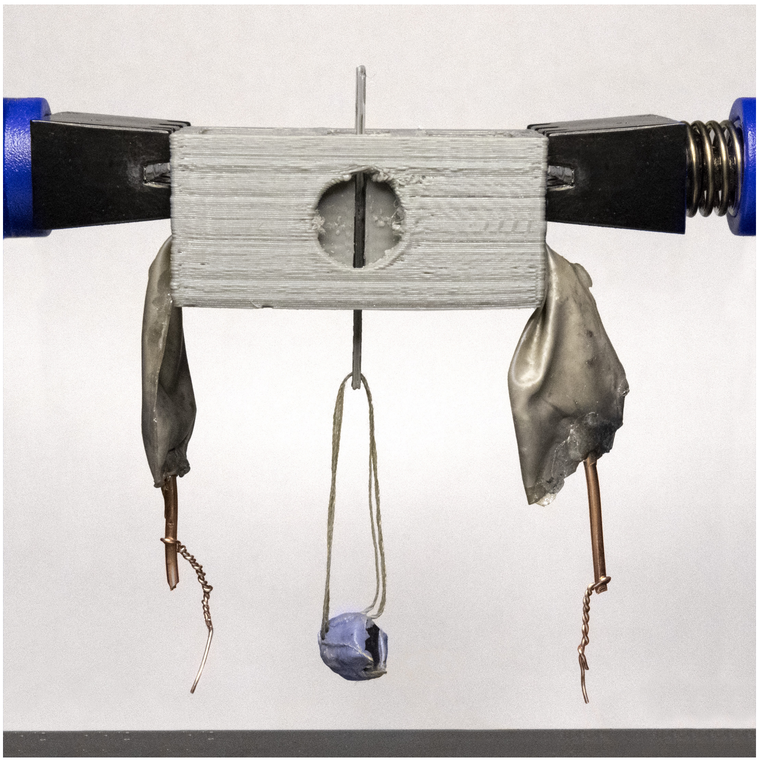

Figure 4.5: Test of second implementation.

The linkage solution proposed needs a compressible fluid in order to not hinder the membrane movements because surface deformation. The implemented actuator use air as that compressible fluid, which is present in the linkage solution as bubbles. These air bubbles generate a variation in resistance of the actuator which entails variability in measures. The lower effective field calculated was $B_e = 0.3\ T$.

The maximum weight Lorentzito was able to lift was $2.2 \times 10^{-3}\ Kg$. The pulling seems linear since the displacement was apparently constant. It means that friction and elasticity effects are almost zero in the second implementation. It was possible to measure a $t_{max} = 5s$ at $7\ A$, because air bubbles sometimes created tiny paths for electric current generating high Joule losses because of high resistivities in the path of current. That heat break the component melting the latex.

The value of the figures of merit in the experiment conditions, that is $I = 7\ A$ and $l = 3 \times 10^{-3}\ m$, is represented in table 4.1.

Table 4.1: Experimental figures of merit.

$B_e[T]$	$\rho_{\frac{N}{W}}[s/m]$	ρ_m	$\rho[s/m]$	ϵ_v	ϵ_m	$t_{max}[s]$	$I_{max}[A]$
0.3	3.14×10^{-3}	0.17	5.34×10^{-5}	0.14	0.22	5	> 7

It is very interesting to check where the power dissipates. The voltage drop was measured with a $0.01\ V$ precision voltmeter. With this limitation, it was found that at least 87.14% of the power was dissipated in the linkage solution.

Configurations with more than one Lorentzito were not tested. Nevertheless, figures of merit can be calculated for that geometry and materials. Because of the additional weight and resistance added from the ideal Loretnzito, the contour lines are displaced leaving less options to accomplish enough force to lift its own weight. As shown in Figures 4.6a , 4.6b, 4.6c and 4.6d, more than $48A$ are needed to lift its own weight.

Figure 4.6a shows a better power efficiency than in the theoretical analysis shown in Figure 3.5. That is because conductors have more section than l^2 because of construction inaccuracies. Nevertheless, this implementation has a worse behaviour in terms of how many times it is able to lift its own weight as shown in Figure 4.6b. Indeed, in the same intervals of I and l, it is only able to lift itself less than twice as shown in Figure 4.6d. As expected, force-mass-consumption highest rates are clearly shifted to higher sizes and currents in Figure 4.6c than in the superior limit shown in Figure 3.7.

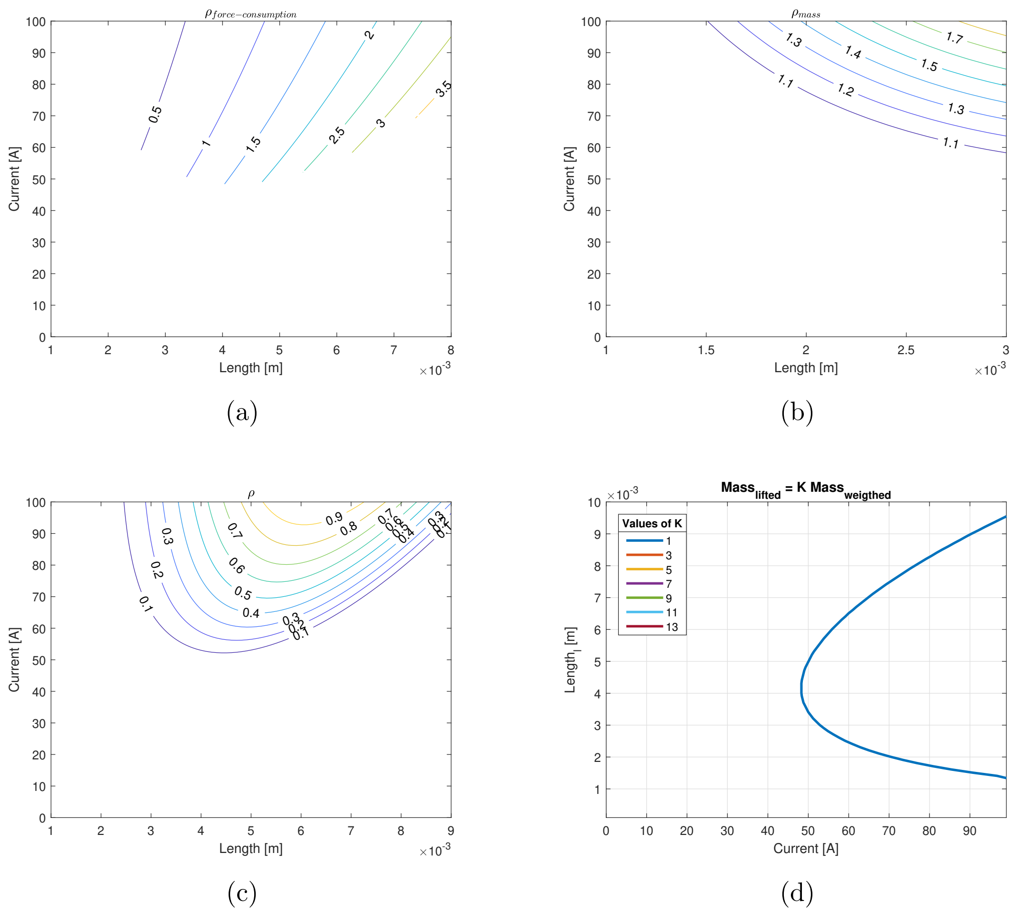

Figure 4.6: (a) $\rho_{\frac{N}{W}}$ force-consumption quotient contour lines at intervals $I \in [0, 100]$ and $l \in [10^{-3}, 80^{-3}]$ for the second implementation, (b) ρ_m mass quotient contour lines at intervals $I \in [0, 100]$ and $l \in [10^{-3}, 30^{-3}]$ for the second implementation, (c) ρ force-mass-consumption quotient contour lines at intervals $I \in [0, 100]$ and $l \in [10^{-3}, 90^{-3}]$ for the second implementation, (d) Times actuator mass is lifted at intervals $I \in [0, 100]$ and $l \in [10^{-3}, 10^{-2}]$ for the second implementation.

The experiment results are far from the ideal Lorentzito but represent a success in terms of proving the concept of a Linear Lorentzito and are coherent with the theoretical development.

Chapter 5

Conclusions and Future Work

5.1 Conclusions

In this thesis, a new linear actuator is proposed to overcome problems found in existing actuators. A theoretical analysis is done to solve its peculiarities. Then, a reference framework is set to test the performance of the proposition and compare it with current solutions.

Magnetic and current density fields of the proposed designs are simulated before the implementation. This practice has saved a lot of time that would have otherwise been wasted in the implementation. Nevertheless, it is impossible to simulate the entire reality in other place and time than reality itself. Either because its complexity or the underestimation of some phenomena, the functionality of a design should be tested in a prototype. That was the case of membranes and fluid dynamics. Membranes, because friction and elasticity were underestimated. The same happened with the behaviour of the liquid electrical conductor near the inner conductor. When the first implementation was tested, it was clear that something was hindering the expected behaviour. Once some explanations were proposed, a second implementation was tested where those phenomena were avoided.

The second implementation shows that its performance is far from the limit set by the ideal Lorentzito. As expected from an early approach to a new designing concept, there is a great potential for improvement. Nevertheless, it is enough to prove the ideas in this thesis. The Lorentz force is a physical phenomena suitable to generate high forces with low energy consumption. Moreover, still theoretically, it seems to be a very good candidate to create small artificial contractive structures if used in the way exposed in this thesis and, perhaps, suitable for the implementation of artificial muscles. Lorentzitos are the tangible counterpart of this asseveration.

5.2 Future Work

The linkage problem has been solved since a functional Loretnzito has been implemented. Nevertheless, some phenomenons hinder its performance. Therefore, future implementations need to be improved. In the first implementation, the pressure field of the liquid metal should be measured or simulated. It would be advisable to have an estimation of how much it worsens the expected behaviour. In the second implementation, the liquid metal is not stable in shape. Its resistivity varies too much, so heating and power dissipation is not accurately predictable. Moreover, membranous solutions may not be the best option, so new ways of solving the linkage problem should be tested.

In this thesis, a single actuator has been designed and tested but Lorentzitos are meant to be grouped playing a coordinated role in motion. The algorithmics and implementations of these behaviours are the natural evolution of this thesis.

Lastly, even Halbach cylinder has been tested good enough, the approximation made of cubic magnets looks improvable. Either using Halbach spheres or refining the approximation, higher magnetic fields and figures of merit could be reached.

Appendix A

Impact

Accordingly to a MarketsandMarkets™research report sample **?**, linear actuators are far more used than rotatory in industrial applications and end use applications. Among all kind of actuators only pneumatic actuators have a bigger market size than electrical actuators. Moreover, the electrical segment is expected to grow at the highest Compound Annual Growth Rate (CAGR). Therefore, the solution presented in this thesis satisfies a tangible necessity and as it offers some alternatives and enhancements, may take its place in the global market of actuators.

- Social impact: this thesis does not represent a direct impact in society since developed knowledge, even it it belongs to applied research, is at a very primitive stage. Nevertheless, it is potentially revolutionary in energy saving. It can also help the motion of people and robots in novel ways if an artificial muscle is finally implemented.

- Economical impact: this thesis will have an impact in the economic field in saving resources as more efficient actuators can be developed. In industrial applications the costs of manufacturing and services can be dropped down using the techniques shown in this thesis. End users of linear actuators would be able to save resources by consuming less energy.

- Ethical impact: this impact is controlled as the experiments performed did not involve living beings. The research was only directed to develop the ideas proposed with no intention other than enhance linear actuators. Therefore, no ethical impact can be analysed based on this thesis.

- Legal impact: all the technologies used during this thesis are properly licensed and legally acquired. An analysis has been done so that not infringement of any law in terms of industrial or intellectual property has been done.

- Environmental impact: RoHS has been scrupulously followed. Metals used in the implementations are not dangerous to living beings or environment. Moreover, PLA is a biodegradable and bioactive polyester.

Appendix B

Budget

This project has been developed during ten months at Laboratorio de Robótica y Control de la E.T.S de Ingenieros de Telecomunicación. The budget is calculated taking into account human resources, software, technical equipment and some material used during the project.

- **Costs derived from human resources**

  People involved in the project are project manager (engineer) and the engineering student, author of this thesis as shown in Table B.1.

Table B.1: Costs derived from human resources.

	Cost per hour (€)	Working hours	Total costs (€)
Project manager	90.00	30	2700.00
Engineering student	60.00	360	21,600.00
TOTAL			**24,300.00€**

- **Costs derived from sofware and technical equipment**

  For this thesis, the software and technical equipment listed on Table B.2 has been used. The total costs are computed by the product of the depreciation cost per month and the time of use.

Table B.2: Costs derived from software and technical equipment.

	Lifetime (years)	Units	Cost (€)	Depreciation (€/month)	Time used (month)	Total cost (€)
Hephestos 2	6	1	850.00	141.00	4	564
Agilent E3646A	10	1	1,100.00	110.00	1	110
Personal Computer	5	1	1200.00	20.00	10	200
MATLAB software	1	1	2,000.00	166.67	2	333.34
Autodesk Inventor software	1	1	2,553.10	212.75	3	638.28
TOTAL						**1,845.62**

- **Costs derived from consumables**

Material used in implementation and tests costs are shown in Table B.3.

Table B.3: Costs derived from consumables.

	Cost (€)
Solenoids	110.00
Magnets	90.00
Latex	20.00
PLA	27.00
Galinstan	50.00
Copper	34.00
TOTAL	**331.00**

Therefore, taking into account both items, the total cost of this Thesis is **26,476.62€**.

Appendix C

Metglass datasheet

Metglas®
www.metglas.com

Magnetic Alloy
2714A (cobalt-based)
Technical Bulletin

Applications

- Switch-mode power supply applications
- High frequency transformers
- High sensitivity matching transformers
- Ultra-sensitive current transformers
- Shielding
- Sensor applications

Benefits

- Extremely low core loss
- Ultra-high permeability
- High squareness ratio – low coercive force
- Near-zero magnetostriction
- Excellent corrosion resistance

Typical DC Hysteresis Loop

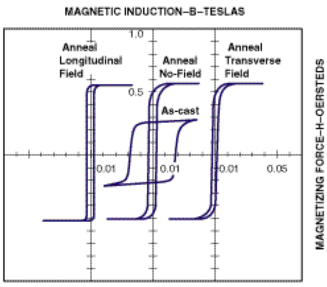

Typical Impedance Permeability Curves, No-Field Anneal

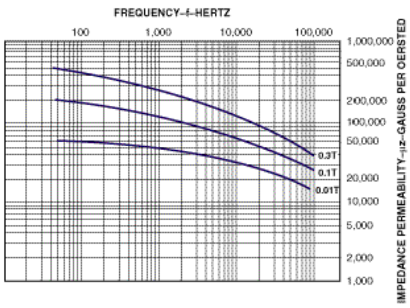

Physical Properties

Density (g/cm^3) 7.59
Vicker's Hardness (50g load) 960
Tensile Strength (GPa) 1-2
Elastic Modulus (GPa) 100-110
Lamination Factor (%) . . . .>75
Thermal Expansion (ppm/°C) 12.7
Crystallization Temperature (°C) 550
Continuous Service Temp. (°C) 90

Magnetic Properties

Saturation Induction (T) 0.57
Maximum D.C. Permeability (μ):
Annealed 1,000,000
As Cast . . . .>80,000
Saturation Magnetostriction (ppm) .. . . <0.5
Electrical Resistivity (μΩ.cm) 142
Curie Temperature (°C) 225

email: *metglas@metglas.com*
1-800-581-7654

Typical Core Loss Curves
Metglas Alloy 2714A

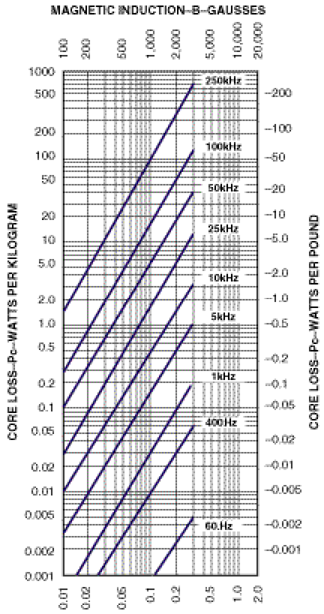

Metglas®
www.metglas.com

Magnetic Alloy 2714A (cobalt-based)
Technical Bulletin

Notes :

Contact Information:

AMERICAS

Metglas®, Inc.

440 Allied Drive
Conway, SC 29526

Tel: (800) 581-7654
Tel: (843) 349-7363
Fax: (843) 349-6815

ASIA

Hitachi Metals Hong Kong

Units 2212-14, 22/F.
Miramar Tower, 132 Nathan Road,
Tsimshatsui, Kowloon
Hong Kong

Tel: 852-27244183
Fax: 852-27227660

EUROPE

Hitachi Metals Europe

Immermannstrasse 14-16
D-40210 Düsseldorf
Germany

Tel :49(0)211-16009-23
Fax:49(0)211-16009-30

Appendix D

Magents datasheet

supermagnete

Ficha técnica del artículo W-03-N

Datos técnicos y seguridad de uso

Webcraft GmbH
Industriepark 206
78244 Gottmadingen, Alemania

Teléfono: +49 7731 939 839 1
Fax: +49 7731 939 839 9

www.supermagnete.es
support@supermagnete.es

1. Datos técnicos

Cód. artículo	W-03-N
Material	NdFeB
Forma	Cubo
Longitud del lado	3 mm
Tolerancia	+/- 0,1 mm
Revestimiento	niquelado (Ni-Cu-Ni)
Tipo de fabricación	sinterizado
Magnetización	N45
fza. sujec.	aprox. 290 g (aprox. 2,84 N)
Temperatura de servicio máx.	80°C
Peso	0,2052 g
Temperatura de Curie	310 °C
Remanencia Br	13200-13700 G, 1.32-1.37 T
Coercitividad bHc	10.8-12.5 kOe, 860-995 kA/m
Coercitividad iHc	≥12 kOe, ≥955 kA/m
Producto energético (BxH)max	43-45 MGOe, 342-358 kJ/m^3

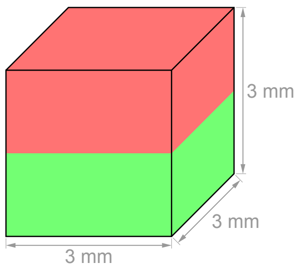

Sin sustancias nocivas conforme a la directiva RoHS 2011/65/UE.

2. Advertencias

Peligro

Ingestión

Los niños pueden tragarse los imanes pequeños.
En caso de haber tragado varios imanes, éstos se pueden fijar en el intestino y causar complicaciones mortales.

¡Los imanes no son juguetes! Asegúrese de mantenerlos fuera del alcance de los niños.

Peligro

Conductividad eléctrica

Los imanes están hechos de metal y son conductores de corriente eléctrica.
Si los niños intentan meter un imán en un enchufe, podrían electrocutarse.

¡Los imanes no son juguetes! Asegúrese de mantenerlos fuera del alcance de los niños.

Advertencia	Fragmentos metálicos
	Los imanes de neodimio son frágiles. Si dos imanes chocan, pueden saltar fragmentos. Los fragmentos afilados pueden salir despedidos a varios metros de distancia y causar lesiones oculares.
	• Evite que los imanes choquen entre sí. • Si va a manipular imanes grandes, póngase unas gafas protectoras. • Asegúrese de que las personas a su alrededor estén protegidas de igual modo o se mantengan a una distancia prudente.

3. Manejo y almacenamiento

Atención	Campo magnético
	Los imanes generan un campo magnético fuerte y de gran alcance, por lo que algunos dispositivos podrían estropearse, como por ejemplo: televisores, ordenadores portátiles, discos duros, tarjetas de crédito, soportes de datos, relojes mecánicos, audífonos y altavoces.
	• Mantenga los imanes alejados de todos aquellos objetos y dispositivos que puedan estropearse debido a campos magnéticos fuertes. • Tenga en cuenta nuestra tabla de distancias recomendadas: www.supermagnete.es/faq/distance

Atención	Inflamabilidad
	Si los imanes se mecanizan, el polvo de perforación se puede inflamar fácilmente.
	Evite este tipo de mecanizado de los imanes o utilice una herramienta adecuada y agua refrigerante en abundancia.

Atención	Alergia al níquel
	La mayoría de nuestros imanes contiene níquel, incluso los que no llevan revestimiento de níquel. • Algunas personas tienen reacciones alérgicas al entrar en contacto con el níquel. • Las alergias al níquel se pueden desarrollar debido al contacto continuado con objetos que contienen níquel.
	• Evite que la piel entre en contacto con imanes de forma continuada. • No haga uso de imanes si ya tiene alergia al níquel.

Aviso	Efecto sobre las personas
	Según los conocimientos actuales, los campos magnéticos de imanes permanentes no tienen ningún efecto positivo o negativo apreciable sobre las personas. Es muy improbable que el campo magnético de un imán permanente pueda suponer un riesgo para la salud, pero no se puede excluir del todo.
	• Por su seguridad, evite el contacto continuo con imanes. • Mantenga los imanes grandes al menos a un metro de distancia de su cuerpo.

Aviso	Fragmentación del revestimiento
	La mayor parte de nuestros imanes de neodimio dispone de un revestimiento fino de níquel-cobre-níquel para protegerlos de la corrosión. Este revestimiento puede fragmentarse o resquebrajarse al ser golpeado o expuesto a grandes presiones. Esto provoca que los imanes se hagan más sensibles ante condiciones ambientales como la humedad, pudiendo llegar a oxidarse.
	• Separe los imanes grandes, especialmente las esferas, con ayuda de un trozo de cartón. • Evite que los imanes choquen entre sí, así como las cargas mecánicas continuadas (p. ej. impactos).

Aviso	Oxidación, corrosión, herrumbre
	Los imanes de neodimio no tratados se oxidan muy rápidamente y se deshacen. La mayor parte de nuestros imanes dispone de un revestimiento fino de níquel-cobre-níquel para protegerlos de la corrosión. Este revestimiento también ofrece cierta protección frente a la corrosión, pero no resulta lo suficientemente resistente en caso de un uso continuado en espacios exteriores.
	• Utilice los imanes tan sólo en espacios interiores secos o protéjalos de las condiciones ambientales. • Evite dañar el revestimiento.

Aviso	Resistencia a la temperatura
	Los imanes de neodimio tienen una temperatura de uso máxima de entre 80 y 200 °C. La mayor parte de los imanes de neodimio pierde parte de su fuerza de sujeción de manera permanente a partir de los 80 °C.
	• No utilice los imanes en aquellos lugares donde vayan a estar expuestos a temperaturas altas. • Si utiliza pegamento, evite endurecerlo con aire caliente.

Aviso	Mecanizado
	Los imanes de neodimio son frágiles, termosensibles y se oxidan fácilmente. • Los imanes se pueden fragmentar si se utiliza una herramienta inadecuada a la hora de perforarlos o serrarlos. • Los imanes se pueden desmagnetizar como consecuencia del calor producido. • Si el revestimiento está dañado, el imán se oxida y se deshace.
	Evite el procesamiento mecánico de los imanes si no dispone de la experiencia y máquinas necesarias.

4. Instrucciones para el transporte

Atención	Transporte aéreo
	Los campos magnéticos de los imanes embalados de manera inadecuada pueden alterar el funcionamiento de los dispositivos de navegación de los aviones. En el peor de los casos, se podría producir un accidente.
	• En caso de transporte aéreo, envíe los imanes única y exclusivamente en embalajes con suficiente protección magnética. • Tenga en cuenta las normas correspondientes: www.supermagnete.es/faq/airfreight

Atención	Envíos postales
	Los campos magnéticos de los imanes embalados de manera inadecuada pueden provocar daños en los dispositivos de clasificación postal, así como en las mercancías frágiles de otros embalajes.
	• Tenga en cuenta nuestros consejos para el envío: www.supermagnete.es/faq/shipping • Utilice una caja con el suficiente espacio y coloque los imanes en el centro del embalaje con ayuda de material de relleno. • Coloque los imanes en el embalaje de manera que los campos magnéticos se neutralicen entre sí. • Utilice placas de acero para proteger del campo magnético, en caso necesario. • Para el transporte aéreo, se aplican normas más estrictas: tenga en cuenta las advertencias para el "transporte aéreo".

5. Instrucciones para una correcta eliminación

Las cantidades pequeñas de imanes de neodimio gastados se pueden depositar en la basura común. Las cantidades mayores de imanes se deben llevar a los puntos de recogida de residuos metálicos.

6. Disposiciones legales

Nuestros imanes de neodimio no están destinados a la distribución/exportación a EEUU, Canadá y Japón. Por ello, queda expresamente prohibido exportar de manera directa o indirecta a los países indicados anteriormente los imanes de neodimio suministrados por nosotros o los productos finales elaborados con estos imanes.

Código TARIC: 8505 1100 65 0

Origen: China

Para más información sobre imanes, consulte la página
www.supermagnete.es/faq.php

Fecha de los datos: 23.11.2011